number of nerve fibers is reduced in the ventral spinal nerve root, reflecting motor neuronopathy. Sensory neurons in the dorsal root ganglia were less severely affected, and large myelinated fibers demonstrate a distally accentuated sensory axonopathy in the peripheral nervous system. Neurons in the Onufrowicz nuclei, intermediolateral columns, and Clarke's columns of the spinal cord are generally well preserved. Muscle histopathology includes both neurogenic and myogenic findings: there are groups of atrophic fibers with a number of small angular fibers, fiber type grouping and clamps of pyknotic nuclei as well as variability in fiber size, hypertrophic fibers, scattered basophilic regenerating fibers, and central nuclei (Figs. 1B and C).

A pathologic hallmark of polyglutamine diseases is the presence of nuclear inclusions (NIs). In SBMA, NIs containing the pathogenic AR are found in the residual motor neurons in the brainstem and spinal cord as well as in nonneuronal tissues including prostate, testis, and skin (Li et al., 1998). These inclusions are detectable using antibodies recognizing a small portion of the N-terminus of the AR protein, but not by those against the C-terminus of the protein. This observation implies that the C-terminus of AR is truncated or masked upon formation of NI. A full-length AR protein with expanded polyglutamine tract is cleaved by caspase-3, liberating a polyglutamine-containing toxic fragment, and the susceptibility to cleavage is polyglutamine repeat length-dependent (Kobayashi et al., 1998). Thus, proteolytic cleavage is likely to enhance the toxicity of the pathogenic AR protein. Electron microscopic immunohistochemistry shows dense aggregates of AR-positive granular material without limiting membrane, both in the neural and nonneural inclusions, in contrast to the other polyglutamine diseases in which NIs take the form of filamentous structures. Although NI is a disease-specific histopathological finding, its role in pathogenesis has been heavily debated. Several studies have suggested that NI may indicate cellular response coping with the toxicity of abnormal polyglutamine protein (Arrasate et al., 2004). Instead, the diffuse nuclear accumulation of the mutant protein has been considered essential for inducing neurodegeneration in polyglutamine diseases including SBMA.

An immunohistochemical study on autopsied SBMA patients using an anti-polyglutamine antibody demonstrates that diffuse nuclear accumulation of the pathogenic AR is more frequently observed than NIs in the anterior horn of spinal cord (Adachi et al., 2005). Intriguingly, the frequency of diffuse nuclear accumulation of the pathogenic AR in spinal motor neurons strongly correlates with the length of the CAG repeat in the AR gene. No such correlation has been found between NI occurrence and the CAG repeat length. Similar findings have also been reported on other polyglutamine diseases. Taken together, it appears that the pathogenic AR containing an elongated polyglutamine tract principally accumulates within the nuclei of motor neurons in a diffusible form, leading to neuronal dysfunction and eventual cell death. In support of this hypothesis, neuronal dysfunction is halted by genetic modulation preventing nuclear import of the pathogenic polyglutamine-containing protein in cellular and animal models of polyglutamine diseases (Gatchel and Zoghbi, 2005).

Since human AR is widely expressed in various organs, nuclear accumulation of the pathogenic AR protein is detected not only in the central nervous system but also in nonneuronal tissues such as scrotal skin (Figs. 1D and E). The degree of pathogenic AR accumulation in scrotal skin epithelial cells tends to be correlated with that in the spinal motor neurons in autopsy specimens, and it is well correlated with CAG repeat length and inversely correlated with the motor functional scale (Banno et al., in press). These findings indicate that scrotal skin biopsy with anti-polyglutamine immunostaining is a potent biomarker with which to monitor SBMA pathogenic processes. Since SBMA is a slowly progressive disorder, appropriate biomarkers would help improve the power and cost effectiveness of longitudinal clinical treatment trials.

Molecular pathogenesis and therapeutic strategies

Ligand-dependent pathogenesis in animal models of SBMA

SBMA is unique among polyglutamine diseases in that the pathogenic protein, AR, has a specific ligand, testosterone, which alters the subcellular localization of the protein by favoring its nuclear uptake. AR is normally confined to a multi-heteromeric inactive complex in the cell cytoplasm and translocates into the nucleus in a ligand-dependent manner. This ligand-dependent intracellular trafficking of AR appears to play important roles in the pathogenesis of SBMA.

In order to investigate ligand effect in SBMA, we generated transgenic mice expressing the full-length human AR containing 24 or 97 CAGs under the control of a cytomegalovirus enhancer and a chicken β-actin promoter (Katsuno et al., 2002). This model recapitulated not only the neurologic disorder but also the phenotypic difference with gender which is a specific feature of SBMA. The mice with 97CAGs (AR-97Q) exhibited progressive motor impairment, although those with 24 CAGs did not show any manifested phenotypes. Affected AR-97Q mice demonstrated small body size, short life span, progressive muscle atrophy, and weakness as well as reduced cage activity, all of which were markedly pronounced and accelerated in the male AR-97Q mice, but either not observed or far less severe in the female AR-97Q mice. The onset of motor impairment detected by the rotarod task was at 8 to 9 weeks of age in the male AR-97Q mice while 16 weeks or more in the females. The 50% mortality ranged from 66 to 132 days of age in the male AR-97Q mice, whereas mortality of the female AR-97Q mice remained only 10 to 30% at more than 210 days. Western blot analysis revealed the transgenic AR protein smearing from the top of the gel in the spinal cord, cerebrum, heart, muscle, and pancreas. Although the male AR-97Q mice had more smearing protein than their female counterparts, the female AR-97Q mice had more monomeric AR protein. The nuclear fraction contained the most of smearing pathogenic AR protein. Diffuse nuclear staining and less frequent NIs detected by 1C2, an antibody specifically recognizing the expanded polyglutamine tract, were demonstrated in the neurons of spinal cord, cerebrum, cerebellum, brainstem, and dorsal root ganglia as well as in nonneuronal tissues such as heart, muscle, and pancreas. Male AR-97Q mice showed markedly more abundant diffuse nuclear staining and NIs than females, in agreement with the symptomatic and Western blot profile differences with gender. Despite the profound sexual difference of the pathogenic AR protein expression, there was no significant difference in the expression of the transgene mRNA between the male and female AR-97Q mice. These observations indicate that the testosterone level plays important roles in the sexual difference of phenotypes, especially in the post-transcriptional stage of the pathogenic AR.

The dramatic sexual difference of phenotypes led us to hormonal interventions in our mouse model. First, we castrated male AR-97Q mice in order to decrease their testosterone level. Castrated male AR-97Q mice showed profound improvement of symptoms, histopathologic findings, and nuclear localization of the pathogenic AR compared with the sham-operated male AR-97Q mice. Body weight, motor function, and lifespan of male AR-97Q mice were significantly improved by castration. Western blot analysis and histopathology revealed diminished nuclear accumulation of the pathogenic AR in the castrated male AR-97Q mice. Next, we administered testosterone to the female AR-97Q mice. In contrast to castration of the male mice, testosterone caused significant aggravation of symptoms, histopathologic features, and nuclear localization of the pathogenic AR in the female AR-97Q mice. Since the nuclear translocation of AR is ligand-dependent, testosterone appears to show toxic effects in the female AR-97Q mice by accelerating nuclear translocation of the pathogenic AR. On the contrary, castration prevented the nuclear localization of the pathogenic AR by reducing the testosterone level. The nuclear accumulation of the pathogenic AR protein with an expanded polyglutamine tract is likely essential in inducing neuronal cell dysfunction and degeneration in the majority of polyglutamine diseases. It thus appears logical that reduction in testosterone level improves phenotypic expression by preventing nuclear localization of the pathogenic AR. In support of this hypothesis, the ligand-dependent neurodegeneration has also been revealed in a fruit fly model of SBMA (Takeyama et al., 2002). Alternatively, castration may enhance protective effects of molecular chaperones, which are normally associated with AR and dissociate upon ligand binding.

Testosterone blockade therapy for SBMA

Successful treatment of AR-97Q mice with castration inspired us testosterone blockade therapies using leuprorelin and flutamide (Katsuno et al., 2003). Leuprorelin is a potent luteinizing hormone-releasing hormone (LHRH) analog suppressing the releases of gonadotrophins, luteinizing hormone and follicle-stimulating hormone. This drug has been used for a variety of sex hormone-dependent diseases including prostate cancer, endometriosis, and prepuberty. The primary pharmacological target of leuprorelin is the anterior pituitary. Through its agonizing effect on LHRH-releasing cells, it initially promotes the releases of gonadotrophins, resulting in transient increase in the serum level of testosterone or estrogens. After this surge, the continued use of this drug induces desensitization of the pituitary by reducing LHRH receptor binding sites and/or uncoupling of receptors from intracellular processes. Within about 2 to 4 weeks of leuprorelin administration, human serum testosterone level decreases to the extent achieved by surgical castration. The effects are maintained during the treatment, suggesting that continuous administration of leuprorelin is required for its clinical use. This drug thus has been provided as sustained release depot taking the form of polymer microspheres. On the other hand, flutamide, the first discovered androgen antagonist, has highly specific affinity for AR and competes with testosterone for binding to the receptor. It has been used for the treatment of prostate cancer, usually in association with an LHRH analog, in order to block the action of adrenal testosterone. Although flutamide suppresses the androgen-dependent transactivation, it does not reduce the plasma levels of testosterone.

Leuprorelin successfully inhibited nuclear accumulation of the pathogenic AR, resulting in marked amelioration of neuromuscular phenotypes seen in the male AR-97Q mice (Fig. 2). Leuprorelin initially increased the serum testosterone level by agonizing the LHRH receptor but subsequently reduced it to undetectable levels. Androgen blockade effects were also confirmed by reduced weights of the prostate and seminal vesicle. The leuprorelin-treated AR-97Q mice showed longer lifespan, larger body size, and better motor performance compared with vehicle-treated mice. Although leuprorelin-induced infertility was prevented by dose reduction, the therapeutic effects on neuromuscular phenotypes were insufficient at a lower dose of leuprorelin. In the Western blot analysis and anti-polyglutamine immunohistochemistry, the leuprorelin-treated male AR-97Q mice demonstrated a markedly diminished amount of the pathogenic AR in the nucleus, suggesting that leuprorelin successfully reduced nuclear AR accumulation. Testosterone, which was given from 13 weeks of age, markedly aggravated neurological symptoms and pathologic findings of leuprorelin-treated male AR-97Q mice. Leuprorelin appears to improve neuronal dysfunction by preventing ligand-dependent nuclear translocation of the pathogenic AR in the same way as castration. Given its minimal invasiveness and established safety, leuprorelin appears to be a promising therapeutic agent for SBMA. In a preliminary open trial, 6-month treatment with leuprorelin significantly diminished nuclear accumulation of pathogenic AR in the scrotal skin of patients, suggesting that androgen deprivation intervenes in the pathogenic process of human SBMA, as demonstrated in animal studies (Banno et al., in press). Another trial on a larger scale is currently underway to verify clinical benefits of leuprorelin for SBMA patients.

Leuprorelin-treated AR-97Q mice showed deterioration of body weight and rotarod task at the age of 8–9 weeks, when serum testosterone initially increased through the agonistic effect of leuprorelin. This change was transient and followed by sustained amelioration along with consequent suppression of testosterone production. The foot print analysis also revealed temporary exacerbation of motor impairment. Immunostaining of tail specimen, sampled from the same individual mouse, demonstrated an increase in the number of the muscle fibers with nuclear 1C2 staining at 4 weeks of leuprorelin administration,

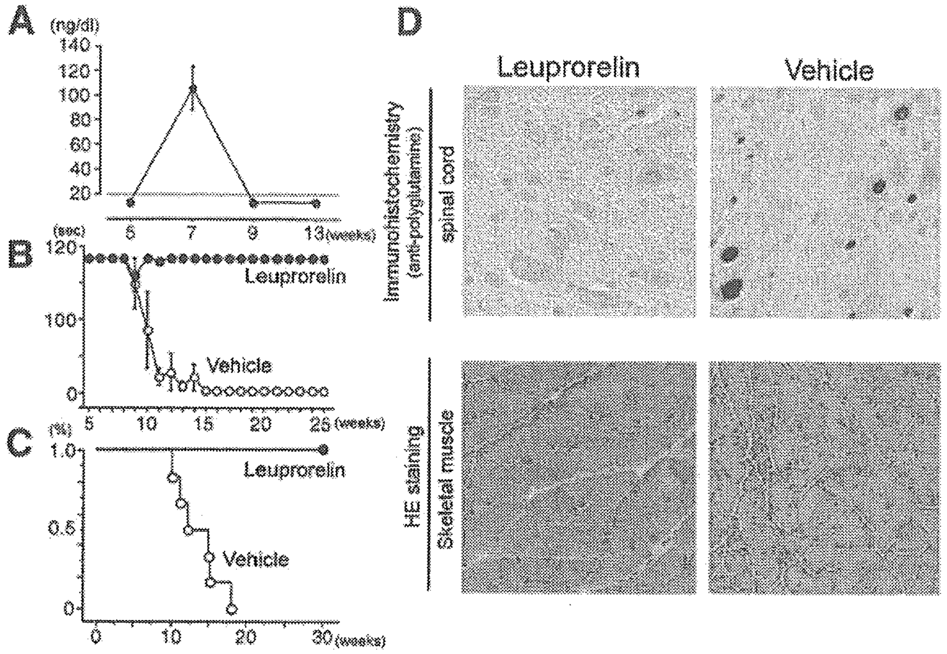

Fig. 2. Effects of leuprorelin on mutant androgen receptor (AR) expression and neuropathology of male AR-97Q mice. (A) Serum testosterone level in AR-97Q mice. Leuprorelin initially increased serum testosterone level but subsequently reduced it to undetectable levels. (B and C) Rotarod task (B) and survival rate (C) of the AR-97Q mice. Leuprorelin markedly improved motor function of the mice at the dose. (D) Immunohistochemistry using 1C2 showed marked differences in diffuse nuclear staining and nuclear inclusions between the leuprorelin-treated and vehicle-treated AR-97Q male mice in the spinal anterior horn. HE staining of the muscle in the vehicle-treated male mouse revealed apparent grouped atrophy and small angulated fibers, which were not seen in the leuprorelin-treated mice.

although this 1C2 staining was diminished by another 4 weeks of treatment. Our results indicate that preventing nuclear translocation of the pathogenic AR is enough to reverse both symptomatic and pathologic phenotypes in our AR-97Q mice. In support with these observations, testosterone deprivation by means of castration reverses motor dysfunction in another transgenic mouse model of SBMA showing fairly slow progression (Chevalier-Larsen et al., 2004). Since the pathophysiology of AR-97Q mice is neuronal dysfunction without neuronal cell loss, our results indicate that the pathogenesis of polyglutamine diseases is reversible at least in its initial stage. From therapeutic point of view, it is of importance to determine the early dysfunctional period in the natural history of human SBMA.

By contrast, flutamide, AR antagonist, did not ameliorate symptoms, pathologic features, or nuclear localization of the pathogenic AR in the male AR-97Q mice, although there was no significant difference in the androgen blockade effects between flutamide and leuprorelin. Flutamide does not inhibit, but may even facilitate, the nuclear translocation of AR. In *consistency* with mouse study, this AR antagonist also promotes nuclear translocation of the pathogenic AR containing an expanded polyglutamine in cellular and fly models of SBMA (Takeyama et al., 2002; Walcott and Merry, 2002). This appears to be the reason why flutamide demonstrated no therapeutic effect in our transgenic mouse model of SBMA. Flutamide is not likely to be a proper therapeutic agent for SBMA.

The castrated or leuprorelin-treated AR-97Q mice showed phenotypes similar to those seen in the female AR-97Q mice, implying that motor impairment of SBMA patients can be reduced to the level in females. SBMA has been considered an X-linked disease, whereas other polyglutamine diseases show autosomal dominant inheritance. In fact, SBMA female patients hardly manifest clinical phenotypes, although they *possess* similar number of a CAG repeat in the disease allele of AR gene as their siblings with SBMA (Sobue et al., 1993; Mariotti et al., 2000). Reduction in the mutant AR expression due to X-inactivation may prevent females from disease manifestation, but hormonal intervention studies using mouse and fly models clearly suggest that low level of testosterone prevents nuclear accumulation of the pathogenic AR protein, resulting in a lack of neurological phenotypes in the females. This view is strongly supported by the observation that manifestation of symptoms is minimal even in homozygous females of SBMA (Schmidt et al., 2002). Therefore, it seems inappropriate to regard SBMA as an X-recessive inherited disease, but rather its neurological phenotype is likely to depend on testosterone concentration.

Role of heat shock proteins in pathogenesis of SBMA

Many components of ubiquitine-proteasome and molecular chaperones are known to colocalize with polyglutamine-containing NIs, implying that failure of cellular defense mechanism underlies neurodegeneration in polyglutamine diseases. Heat shock protein (HSP), a stress-inducible molecular chaperone, is another key to elucidation of the pathogenesis of SBMA. HSPs are classified into different families according to molecular size: Hsp100, Hsp90, Hsp70, Hsp60, Hsp40, and small HSPs (Macario and Conway de Macario, 2005). These HSPs are either constitutively expressed or inducibly synthesized after cellular stress. HSPs play a crucial role in maintaining correct folding, assembly, and intracellular transport of proteins.

For example, Hsp70 and Hsp90, essential components of AR-chaperone complex in the cell cytoplasm, regulate function, nuclear translocation, and degradation of AR (Heinlein and Chang, 2001). Under toxic conditions, HSP synthesis is rapidly upregulated, and nonnative proteins are refolded as a consequence. Therefore, HSPs have attracted a great deal attention as cytoprotective agents against detrimental conditions including ischemia and malignancy.

Several studies suggest that polyglutamine elongation interferes with the protective cellular responses against cytotoxic stress (Wyttenbach, 2004). Truncated AR with an expanded polyglutamine tract delays the induction of Hsp70 after heat shock (Cowan et al., 2003). The threshold of HSP induction is known to be relatively high in spinal motor neurons (Batulan et al., 2003). Expression levels of HSPs are decreased in the brain lesion of an animal model of HD and in that of the SBMA mouse (Hay et al., 2004; Katsuno et al., 2005). Taken together, impairment of HSP induction capability is implicated in the pathogenesis of motor neuron degeneration in SBMA. Not only are HSPs implicated in the pathogenesis of neurodegeneration, but they are also potent suppressors of polyglutamine toxicity. There is increasing evidence that HSPs abrogate polyglutamine-mediated cytotoxicity by refolding and solubilizing the pathogenic proteins (Wyttenbach, 2004; Muchowski and Wacker, 2005). Hsp70 cooperates with Hsp40 in functioning as a molecular chaperone. These HSPs are proposed to prevent the initial conformation conversion of abnormal polyglutamine-containing protein from a random coil to a β-sheet, leading to attenuation of toxic oligomer formation (Wyttenbach, 2004). Overexpression of Hsp70, together with Hsp40, inhibits toxic accumulation of abnormal polyglutamine-containing protein and suppresses cell death in a variety of cellular models of polyglutamine diseases including SBMA (Kobayashi et al., 2000). Hsp70 has also been shown to facilitate proteasomal degradation of abnormal AR protein in a cell culture model of SBMA (Bailey et al., 2002). The favorable effects of Hsp70 have been verified in studies using mouse models of polyglutamine diseases. Overexpression of the inducible form of human Hsp70 markedly ameliorated symptomatic and histopathological phenotypes of our transgenic mouse model of SBMA (Adachi et al., 2003). These beneficial effects are dependent on Hsp70 gene dosage and correlate with the reduction in the amount of nuclear-localized AR protein. It should be noted that the soluble form of the pathogenic AR was also significantly decreased in amount by Hsp70 overexpression, suggesting the degradation of the pathogenic AR may have been accelerated by overexpression of this molecular chaperone.

Favorable effects obtained by genetic modulation of HSP suggest that pharmacological induction of molecular chaperones might be a promising approach to SBMA and other polyglutamine diseases. Geranylgeranylacetone (GGA), an acyclic isoprenoid compound with a retinoid skeleton, has been shown to strongly induce HSP expression in various tissues (Hirakawa et al., 1996). Oral administration of GGA upregulates the levels of Hsp70, Hsp90, and Hsp105 via activation of heat shock factor-1 in the central nervous system and inhibits nuclear accumulation of the pathogenic AR protein, resulting in amelioration of polyglutamine-dependent neuromuscular phenotypes of SBMA transgenic mice (Katsuno et al., 2005). Given its extremely low toxicity, this compound has been used as an oral anti-ulcer drug. Although a high dose appears to be needed for clinical effects, GGA appears to be a safe and promising therapeutic candidate for polyglutamine-mediated neurodegenerative diseases including SBMA.

Inhibition of Hsp90 is also demonstrated to arrest the neurodegeneration in SBMA mouse (Waza et al., 2005). Hsp90 functions in a multi-chaperone complex, assisting proper folding, stabilization, and assembly of so-called client proteins including various oncoproteins and AR (Pratt and Toft, 2003). The Hsp90-client protein complex is stabilized when it is associated with p23, a cochaperone interacting with Hsp90. Treatment with 17-allylamino geldanamycin (17-AAG), a potent Hsp90 inhibitor, dissociated p23 from the Hsp90-AR complex, and thus facilitated proteasomal degradation of the pathogenic AR in cellular and mouse models of SBMA. 17-AAG thereby inhibits nuclear accumulation of this protein, leading to marked amelioration of motor phenotypes of the SBMA mouse model without detectable toxicity (Fig. 3). Of interest is the finding that the pathogenic AR is preferentially targeted to proteasomal degradation in the presence of 17-AAG compared with wild-type AR. Given a high association between p23 and the AR containing expanded polyglutamine, it appears logical that the pathogenic AR is more dependent on Hsp90 to maintain folding and function than wild-type AR and thus is particularly susceptive to Hsp90 inhibition. 17-AAG is also capable of inducing Hsp70 in cellular and mouse models of SBMA. Collectively, 17-AAG, which is now under clinical trials for a wide range of malignancies, would be a good candidate for treatment of SBMA.

Transcriptional dysregulation in SBMA

Disruption of transcriptional machinery has also been hypothesized to underlie the pathogenesis of polyglutamine diseases (Sugars and Rubinsztein, 2003). Gene expression analysis indicates that transcriptional disruption is an early change in the pathogenesis of mouse models of polyglutamine diseases. Transcriptional coactivators such as CBP are sequestrated into the polyglutamine-containing NIs through protein–protein interaction in mouse models and patients with polyQ diseases (Nucifora et al., 2001). Alternatively, the interaction between transcriptional coactivators and soluble pathogenic protein has also been demonstrated in animal models of polyglutamine diseases as well as in postmortem tissues of patients (Steffan et al., 2001). The expression of genes regulated through CBP-mediated transcription is decreased in mouse models of polyglutamine diseases (Sugars and Rubinsztein, 2003). CBP functions as histone acetyltransferase, regulating gene transcription and chromatin structure. It has been indicated that the histone acetyltransferase activity of CBP is suppressed in cellular models of polyglutamine diseases. Taken together, transcriptional dysregulation due to decrease in histone acetylation is likely to underlie the pathogenesis of neurodegeneration in polyglutamine diseases. This hypothesis is exemplified by our experimental

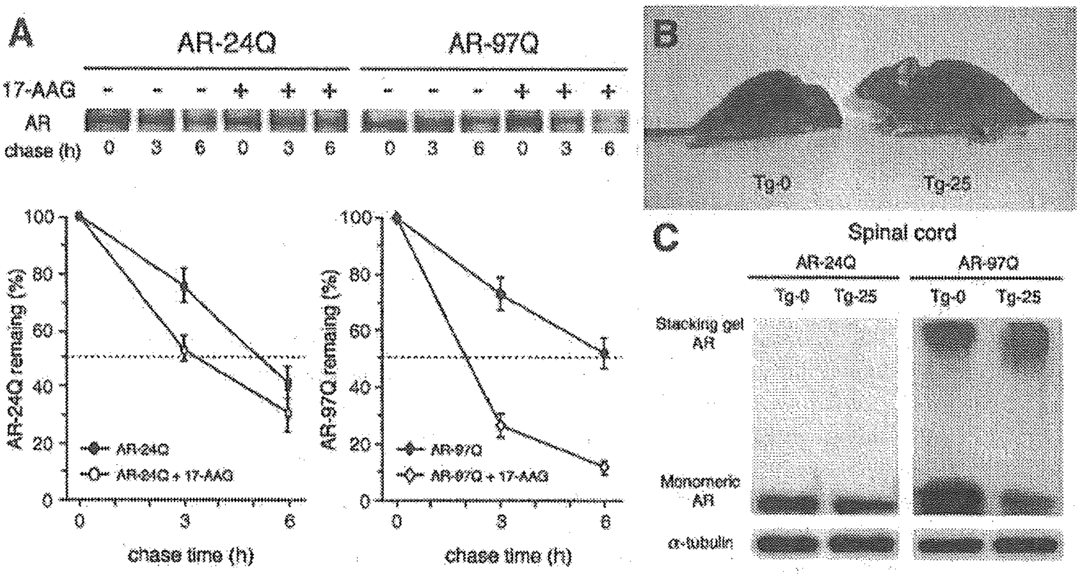

Fig. 3. Effects of 17-AAG on mutant androgen receptor (AR) turnover. (A) Pulse-chase analysis of two forms of AR. The pathogenic AR containing prolonged polyglutamine is degraded more rapidly than the wild-type AR in the presence of 17-AAG. (B) Muscle wasting is obvious in a vehicle-treated SBMA mouse (Tg-0), whereas it is hardly detected in an age-matched SBMA mouse treated with 25 mg/kg of 17-AAG (Tg-25). (C) Western blot analysis of total homogenates from the spinal cord of transgenic mice probed with an anti-AR antibody. 17-AAG decreases the amount of AR in mice bearing the pathogenic AR (AR-97Q), but this effect is only slightly observed in those expressing wild-type AR (AR-24Q).

observation that acetylation of nuclear histone H3 is significantly diminished in SBMA mice (Minamiyama et al., 2004). Additionally, dysfunction of CBP results in a decreased expression of vascular endothelial growth factor in another mouse model of SBMA, indicating the transcriptional alteration is a trigger of neurodegeneration in this disease (Sopher et al., 2004).

Histone acetylation level is determined by interplay between histone acetyltransferase and histone deacetylase (HDAC). Recruitment of HDAC to target genes represses transcription, leading to aberrant cellular function. Since cancellation of HDAC activity results in augmentation of histone acetylation and subsequent restoration of gene transcription, HDAC

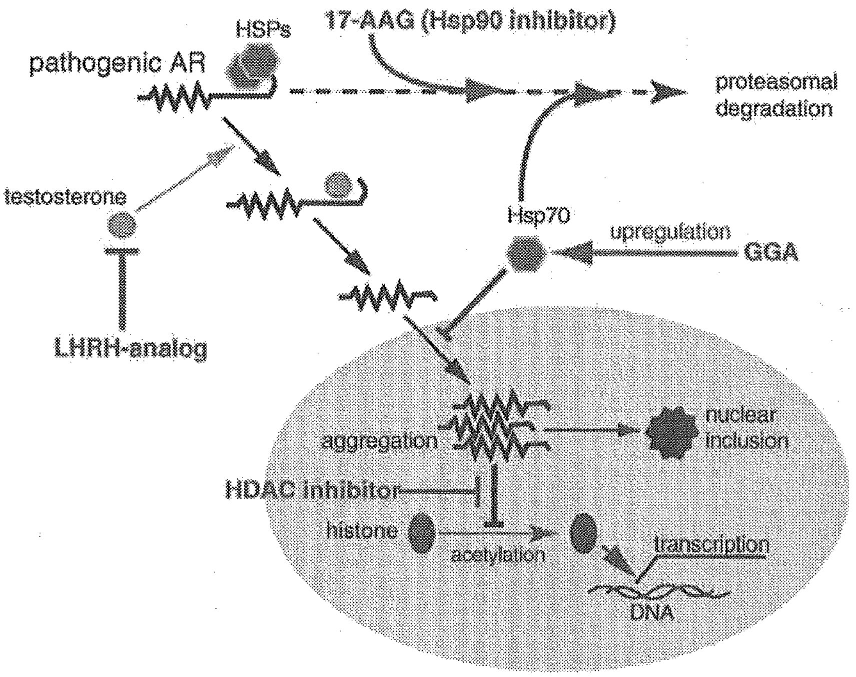

Fig. 4. Pathogenesis-targeting therapeutic approaches to SBMA. In the absence of ligand, the pathogenic AR is confined to a multi-heteromeric inactive complex with heat shock proteins (HSPs) in the cell cytoplasm. Ligand binding facilitates its dissociation from this complex and translocation into the nucleus. In the nucleus, the pathogenic AR forms aggregate and impairs histone acetylation, resulting in transcriptional dysregulation. Several candidates of therapies have been identified on the basis of insights into the molecular mechanisms of the neurodegeneration in SBMA.

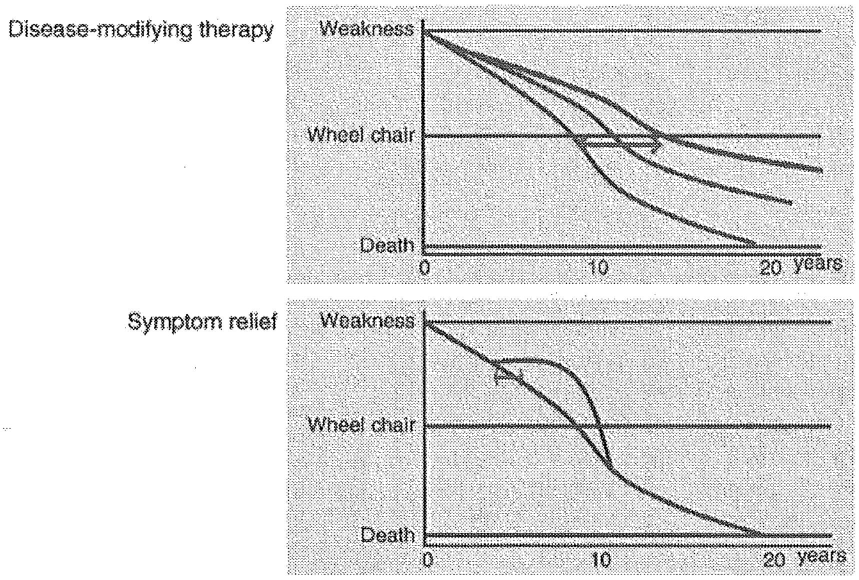

Fig. 5. Disease-modifying therapy and symptom relief. Since the goal of disease-modifying therapy is to inhibit pathogenic progression, long-term trials need to be carried out in order to evaluate drug effects by targeting certain clinical events as the primary endpoint. On the other hand, symptom relief, such as replacement of neurotransmitter, is used to ameliorate symptoms resulting from neurodegeneration. Although trial duration tends to be short, the effect of this therapy is often transient. Arrows indicate trial duration required for each therapy.

inhibitors have been considered to be of therapeutic benefit in polyglutamine diseases (Steffan et al., 2001, Hockly et al., 2003). Butyrate is the first HDAC inhibitor to be discovered, and the related compound, phenylbutyrate, has been successfully employed in experimental cancer therapy. Oral administration of sodium butyrate ameliorates symptomatic and histopathological phenotypes of our mouse model of SBMA through upregulation of histone acetylation in nervous tissues (Minamiyama et al., 2004). Although sodium butyrate is likely to be a promising treatment of SBMA, this compound yielded beneficial effects only within a narrow therapeutic window of dosage in the mouse model. Careful dose determination is mandatory when using HDAC inhibitors for treatment of polyglutamine diseases.

Axonal trafficking defects in SBMA

Motor neurons possess extremely long axon along which molecular motors transport essential components such as organelles, vesicles, cytoskeletons, and signal molecules. This implies that axonal trafficking plays a fundamental role in maintenance of normal function of motor neurons. Obstruction of axonal transport has gained attention as a cause of neuronal dysfunction in a variety of neurodegenerative diseases including SBMA (Gunawardena and Goldstein, 2005). A mutation in the gene of proteins regulating axonal trafficking, dynein and dynactin 1, has been shown to cause motor neuron degeneration in both human and rodent (Puls et al., 2003; Hafezparast et al., 2003). Experimental data suggest that axonal transport might be retarded by pathogenic polyglutamine-containing AR (Szebenyi et al., 2003). Although this notion is intriguing, its contribution to the pathogenesis of SBMA should be further investigated, since aggregation of the pathogenic AR is rarely found within the axon of motor neurons in patients or model mice.

Clinical application of potential therapeutics

Analysis of cellular and animal models provides insight into mechanisms involved in neurodegeneration of SBMA and indicates retinal therapeutic approaches to this disease (Fig. 4). Therapeutic agent candidates for SBMA are grossly classified into two groups: (i) drugs inhibiting accumulation of the pathogenic AR protein and (ii) drugs mitigating downstream pathological events including

Table1
Summary of therapeutic trials in SBMA mouse models

Treatment	Number of mice (per treatment group)	Increase in survival (%)	Rotarod task	Body weight	AR accumulation	Reference
Castration	6	>120%	Improved	Improved	Decreased	Katsuno et al. (2002)
Castration [a]	8–9	Not determined	Improved	No effect	Decreased	Chevalier-Larsen et al. (2004)
Leuprorelin	6	>130%	Improved	Improved	Decreased	Katsuno et al. (2003)
Flutamide	6	No effect	No effect	No effect	No effect	Katsuno et al. (2003)
Sodium butyrate	12–15	56%	Improved	Improved	No effect	Minamiyama et al. (2004)
17-AAG	27	>60%	Improved	Improved	Decreased	Waza et al. (2005)
GGA	12–15	>60%	Improved	Improved	Decreased	Katsuno et al. (2005)

[a] Treatment is initiated after the onset of motor impairment. AR, androgen receptor; 17-AAG, 17-allylamino geldanamycin; GGA, geranylgeranylacetone.

transcriptional dysregulation. The ideal therapy for polyglutamine diseases appears to be a combination of these potential therapeutic strategies, since each drug has potential adverse effects when used in a long term (Agrawal et al., 2005). In addition to pharmacological approaches, genetic interventions such as RNA interference can be applied if safety and delivery problems are solved (Caplen et al., 2002).

Since various therapeutic strategies for SBMA have emerged thanks to animal models recapitulating human diseases, it is of utmost importance to pursue intensive clinical studies to verify the results from animal studies (Table 1). When we apply candidate agents for patients, it should be considered that the majority of therapeutics emerging form animal studies are disease-modifying therapy, but not symptom-relief (Fig. 5). Given that SBMA is a slowly progressive disease, extremely long-term clinical trials are likely necessary to verify clinical benefits of disease-modifying therapies by targeting clinical endpoints such as occurrence of aspiration pneumonia or becoming wheelchair-bound. Suitable surrogate endpoints, which reflect the pathogenesis and severity of SBMA, are thus substantial to assess the therapeutic efficacy in drug trials. To this end, appropriate biomarkers should be identified and validated in translational researches.

Acknowledgments

Fig. 2 is reproduced from Katsuno et al., "Leuprorelin rescues polyglutamine-dependent phenotypes in a transgenic mouse model of spinal and bulbar muscular atrophy (SBMA)" Nat. Med. 9: 768–773, 2003. Fig. 3 is reproduced from Waza et al., "17-AAG, an Hsp90 inhibitor, ameliorates polyglutamine-mediated motor neuron degeneration" Nat. Med. 11: 1088–1095, 2005. This work was supported by a Center-of-Excellence (COE) grant from the Ministry of Education, Culture, Sports, Science and Technology, Japan, and grants from the Ministry of Health, Labour and Welfare, Japan.

References

Adachi, H., Kume, A., Li, M., Nakagomi, Y., Niwa, H., Do, J., Sang, C., Kobayashi, Y., Doyu, M., Sobue, G., 2001. Transgenic mice with an expanded CAG repeat controlled by the human AR promoter show polyglutamine nuclear inclusions and neuronal dysfunction without neuronal cell death. Hum. Mol. Genet. 10, 1039–1048.

Adachi, H., Katsuno, M., Minamiyama, M., Sang, C., Pagoulatos, G., Angelidis, C., Kusakabe, M., Yoshiki, A., Kobayashi, Y., Doyu, M., Sobue, G., 2003. Heat shock protein 70 chaperone overexpression ameliorates phenotypes of the spinal and bulbar muscular atrophy transgenic mouse model by reducing nuclear-localized mutant androgen receptor protein. J. Neurosci. 23, 2203–2211.

Adachi, H., Katsuno, M., Minamiyama, M., Waza, M., Sang, C., Nakagomi, Y., Kobayashi, Y., Tanaka, F., Doyu, M., Inukai, A., Yoshida, M., Hashizume, Y., Sobue, G., 2005. Widespread nuclear and cytoplasmic accumulation of mutant androgen receptor in SBMA patients. Brain 128, 659–670.

Agrawal, N., Pallos, J., Slepko, N., Apostol, B.L., Bodai, L., Chang, L.W., Chiang, A.S., Thompson, L.M., Marsh, J.L., 2005. Identification of combinatorial drug regimens for treatment of Huntington's disease using *Drosophila*. Proc. Natl. Acad. Sci. U. S. A. 102, 3777–3781.

Arrasate, M., Mitra, S., Schweitzer, E.S., Segal, M.R., Finkbeiner, S., 2004. Inclusion body formation reduces levels of mutant huntingtin and the risk of neuronal death. Nature 431, 805–810.

Bailey, C.K., Andriola, I.F., Kampinga, H.H., Merry, D.E., 2002. Molecular chaperones enhance the degradation of expanded polyglutamine repeat androgen receptor in a cellular model of spinal and bulbar muscular atrophy. Hum. Mol. Genet. 11, 515–523.

Banno, H., Adachi, H., Katsuno, M., Suzuki, K., Atsuta, N., Watanabe, H., Tanaka, F., Doyu, M., Sobue, G., in press. Mutant androgen receptor accumulation in SBMA scrotal skin: a pathogenic marker. Ann. Neurol.

Batulan, Z., Shinder, G.A., Minotti, S., He, B.P., Doroudchi, M.M., Nalbantoglu, J., Strong, M.J., Durham, H.D., 2003. High threshold for induction of the stress response in motor neurons is associated with failure to activate HSF1. J. Neurosci. 23, 5789–5798.

Caplen, N.J., Taylor, J.P., Statham, V.S., Tanaka, F., Fire, A., Morgan, R.A., 2002. Rescue of polyglutamine-mediated cytotoxicity by double-stranded RNA-mediated RNA interference. Hum. Mol. Genet. 11, 175–184.

Chevalier-Larsen, E.S., O'Brien, C.J., Wang, H., Jenkins, S.C., Holder, L., Lieberman, A.P., Merry, D.E., 2004. Castration restores function and neurofilament alterations of aged symptomatic males in a transgenic mouse model of spinal and bulbar muscular atrophy. J. Neurosci. 24, 4778–4786.

Clark, P.E., Irvine, R.A., Coetzee, G.A., 2003. The androgen receptor CAG repeat and prostate cancer risk. Methods Mol. Med. 81, 255–266.

Cowan, K.J., Diamond, M.I., Welch, W.J., 2003. Polyglutamine protein aggregation and toxicity are linked to the cellular stress response. Hum. Mol. Genet. 12, 1377–1391.

Doyu, M., Sobue, G., Mukai, E., Kachi, T., Yasuda, T., Mitsuma, T., Takahashi, A., 1992. Severity of X-linked recessive bulbospinal neuronopathy correlates with size of the tandem CAG repeat in androgen receptor gene. Ann. Neurol. 32, 707–710.

Fischbeck, K.H., 1997. Kennedy disease. J. Inherited Metab. Dis. 20, 152–158.

Gatchel, J.R., Zoghbi, H.Y., 2005. Diseases of unstable repeat expansion: mechanism and principles. Nat. Rev., Genet. 6, 743–755.

Gunawardena, S., Goldstein, L.S., 2005. Polyglutamine diseases and transport problems: deadly traffic jams on neuronal highways. Arch. Neurol. 62, 46–51.

Hafezparast, M., Klocke, R., Ruhrberg, C., Marquardt, A., Ahmad-Annuar, A., Bowen, S., Lalli, G., Witherden, A.S., Hummerich, H., Nicholson, S., Morgan, P.J., Oozageer, R., Priestley, J.V., Averillm, S., King, V.R., Ball, S., Peters, J., Toda, T., Yamamoto, A., Hiraoka, Y., Augustin, M., Korthaus, D., Wattler, S., Wabnitz, P., Dickneite, C., Lampel, S., Boehme, F., Peraus, G., Popp, A., Rudelius, M., Schlegel, J., Fuchs, H., Hrabe de Angelis, M., Schiavo, G., Shima, D.T., Russ, A.P., Stumm, G., Martin, J.E., Fisher, E.M., 2003. Mutations in dynein link motor neuron degeneration to defects in retrograde transport. Science 300, 808–812.

Hay, D.G., Sathasivam, K., Tobaben, S., Stahl, B., Marber, M., Mestril, R., Mahal, A., Smith, D.L., Woodman, B., Bates, G.P., 2004. Progressive decrease in chaperone protein levels in a mouse model of Huntington's disease and induction of stress proteins as a therapeutic approach. Hum. Mol. Genet. 13, 1389–1405.

Heinlein, C.A., Chang, C., 2001. Role of chaperones in nuclear translocation and transactivation of steroid receptors. Endocrine 14, 143–149.

Hirakawa, T., Rokutan, K., Nikawa, T., Kishi, K., 1996. Geranylgeranylacetone induces heat shock proteins in cultured guinea pig gastric mucosal cells and rat gastric mucosa. Gastroenterology 111, 345–357.

Hockly, E., Richon, V.M., Woodman, B., Smith, D.L., Zhou, X., Rosa, E., Sathasivam, K., Ghazi-Noori, S., Mahal, A., Lowden, P.A., Steffan, J.S., Marsh, J.L., Thompson, L.M., Lewis, C.M., Marks, P.A., Bates, G.P., 2003. Suberoylanilide hydroxamic acid, a histone deacetylase inhibitor, ameliorates motor deficits in a mouse model of Huntington's disease. Proc. Natl. Acad. Sci. U. S. A. 100, 2041–2046.

Katsuno, M., Adachi, H., Kume, A., Li, M., Nakagomi, Y., Niwa, H., Sang, C., Kobayashi, Y., Doyu, M., Sobue, G., 2002. Testosterone reduction prevents phenotypic expression in a transgenic mouse model of spinal and bulbar muscular atrophy. Neuron 35, 843–854.

Katsuno, M., Adachi, H., Doyu, M., Minamiyama, M., Sang, C., Kobayashi, Y., Inukai, A., Sobue, G., 2003. Leuprorelin rescues polyglutamine-dependent phenotypes in a transgenic mouse model of spinal and bulbar muscular atrophy. Nat. Med. 9, 768–773.

Katsuno, M., Adachi, H., Tanaka, F., Sobue, G., 2004. Spinal and bulbar muscular atrophy: ligand-dependent pathogenesis and therapeutic perspectives. J. Mol. Med. 82, 298–307.

Katsuno, M., Sang, C., Adachi, H., Minamiyama, M., Waza, M., Tanaka, F., Doyu, M., Sobue, G., 2005. Pharmacological induction of heat-shock proteins alleviates polyglutamine-mediated motor neuron disease. Proc. Natl. Acad. Sci. U. S. A. 102, 16801–16806.

Kawahara, H., 1897. A family of progressive bulbar palsy. Aichi. Med. J. 16, 3–4 (in Japanese).

Kennedy, W.R., Alter, M., Sung, J.H., 1968. Progressive proximal spinal and bulbar muscular atrophy of late onset. A sex-linked recessive trait. Neurology 18, 671–680.

Kobayashi, Y., Miwa, S., Merry, D.E., Kume, A., Mei, L., Doyu, M., Sobue, G., 1998. Caspase-3 cleaves the expanded androgen receptor protein of spinal and bulbar muscular atrophy in a polyglutamine repeat length-dependent manner. Biochem. Biophys. Res. Commun. 252, 145–150.

Kobayashi, Y., Kume, A., Li, M., Doyu, M., Hata, M., Ohtsuka, K., Sobue, G., 2000. Chaperones Hsp70 and Hsp40 suppress aggregate formation and apoptosis in cultured neuronal cells expressing truncated androgen receptor protein with expanded polyglutamine tract. J. Biol. Chem. 275, 8772–8778.

La Spada, A.R., Wilson, E.M., Lubahn, D.B., Harding, A.E., Fischbeck, K.H., 1991. Androgen receptor gene mutations in X-linked spinal and bulbar muscular atrophy. Nature 352, 77–79.

Li, M., Miwa, S., Kobayashi, Y., Merry, D.E., Yamamoto, M., Tanaka, F., Doyu, M., Hashizume, Y., Fischbeck, K.H., Sobue, G., 1998. Nuclear inclusions of the androgen receptor protein in spinal and bulbar muscular atrophy. Ann. Neurol. 44, 249–254.

Macario, A.J., Conway de Macario, E., 2005. Sick chaperones, cellular stress, and disease. N. Engl. J. Med. 353, 1489–1501.

Mariotti, C., Castellotti, B., Pareyson, D., Testa, D., Eoli, M., Antozzi, C., Silani, V., Marconi, R., Tezzon, F., Siciliano, G., Marchini, C., Gellera, C., Donato, S.D., 2000. Phenotypic manifestations associated with CAG-repeat expansion in the androgen receptor gene in male patients and heterozygous females: a clinical and molecular study of 30 families. Neuromuscul. Disord. 10, 391–397.

Minamiyama, M., Katsuno, M., Adachi, H., Waza, M., Sang, C., Kobayashi, Y., Tanaka, F., Doyu, M., Inukai, A., Sobue, G., 2004. Sodium butyrate ameliorates phenotypic expression in a transgenic mouse model of spinal and bulbar muscular atrophy. Hum. Mol. Genet. 13, 1183–1192.

Muchowski, P.J., Wacker, J.L., 2005. Modulation of neurodegeneration by molecular chaperones. Nat. Rev., Neurosci. 6, 11–22.

Nucifora Jr., F.C., Sasaki, M., Peters, M.F., Huang, H., Cooper, J.K., Yamada, M., Takahashi, H., Tsuji, S., Troncoso, J., Dawson, V.L., Dawson, T.M., Ross, C. A., 2001. Interference by huntingtin and atrophin-1 with cbp-mediated transcription leading to cellular toxicity. Science 291, 2423–2428.

Poletti, A., 2004. The polyglutamine tract of androgen receptor: from functions to dysfunctions in motor neurons. Front. Neuroendocrinol. 25, 1–26.

Pratt, W.B., Toft, D.O., 2003. Regulation of signaling protein function and trafficking by the hsp90/hsp70-based chaperone machinery. Exp. Biol. Med. 228, 111–133.

Puls, I., Jonnakuty, C., LaMonte, B.H., Holzbaur, E.L., Tokito, M., Mann, E., Floeter, M.K., Bidus, K., Drayna, D., Oh, S.J., Brown Jr., R.H., Ludlow, C.L., Fischbeck, K.H., 2003. Mutant dynactin in motor neuron disease. Nat. Genet. 33, 455–456.

Schmidt, B.J., Greenberg, C.R., Allingham-Hawkins, D.J., Spriggs, E.L., 2002. Expression of X-linked bulbospinal muscular atrophy (Kennedy disease) in two homozygous women. Neurology 59, 770–772.

Sobue, G., Hashizume, Y., Mukai, E., Hirayama, M., Mitsuma, T., Takahashi, A., 1989. X-linked recessive bulbospinal neuronopathy. A clinicopathological study. Brain 112, 209–232.

Sobue, G., Doyu, M., Kachi, T., Yasuda, T., Mukai, E., Kumagai, T., Mitsuma, T., 1993. Subclinical phenotypic expressions in heterozygous females of X-linked recessive bulbospinal neuronopathy. J. Neurol. Sci. 117, 74–78.

Sopher, B.L., Thomas, Jr., P.S., LaFevre-Bernt, M.A., Holm, I.E., Wilke, S.A., Ware, C.B., Jin, L.W., Libby, R.T., Ellerby, L.M., La Spada, A.R., 2004. Androgen receptor YAC transgenic mice recapitulate SBMA motor neuronopathy and implicate VEGF164 in the motor neuron degeneration. Neuron 41, 687–699.

Sperfeld, A.D., Karitzky, J., Brummer, D., Schreiber, H., Haussler, J., Ludolph, A.C., Hanemann, C.O., 2002. X-linked bulbospinal neuropathy: Kennedy disease. Arch. Neurol. 59, 1921–1926.

Steffan, J.S., Bodai, L., Pallos, J., Poelman, M., McCampbell, A., Apostol, B.L., Kazantsev, A., Schmidt, E., Zhu, Y.Z., Greenwald, M., Kurokawa, R., Housman, D.E., Jackson, G.R., Marsh, J.L., Thompson, L.M., 2001. Histone deacetylase inhibitors arrest polyglutamine-dependent neurodegeneration in *Drosophila*. Nature 413, 739–743.

Sugars, K.L., Rubinsztein, D.C., 2003. Transcriptional abnormalities in Huntington disease. Trends Genet. 19, 233–238.

Szebenyi, G., Morfini, G.A., Babcock, A., Gould, M., Selkoe, K., Stenoien, D.L., Young, M., Faber, P.W., MacDonald, M.E., McPhaul, M.J., Brady, S.T., 2003. Neuropathogenic forms of huntingtin and androgen receptor inhibit fast axonal transport. Neuron 40, 41–52.

Takeyama, K., Ito, S., Yamamoto, A., Tanimoto, H., Furutani, T., Kanuka, H., Miura, M., Tabata, T., Kato, S., 2002. Androgen-dependent neurodegeneration by polyglutamine-expanded human androgen receptor in *Drosophila*. Neuron 35, 855–864.

Walcott, J.L., Merry, D.E., 2002. Ligand promotes intranuclear inclusions in a novel cell model of spinal and bulbar muscular atrophy. J. Biol. Chem. 277, 50855–50859.

Waza, M., Adachi, H., Katsuno, M., Minamiyama, M., Sang, C., Tanaka, F., Inukai, A., Doyu, M., Sobue, G., 2005. 17-AAG, an Hsp90 inhibitor, ameliorates polyglutamine-mediated motor neuron degeneration. Nat. Med. 11, 1088–1095.

Wyttenbach, A., 2004. Role of heat shock proteins during polyglutamine neurodegeneration: mechanisms and hypothesis. J. Mol. Neurosci. 23, 69–96.

Mutant Androgen Receptor Accumulation in Spinal and Bulbar Muscular Atrophy Scrotal Skin: A Pathogenic Marker

Haruhiko Banno, MD, Hiroaki Adachi, MD, Masahisa Katsuno, MD, Keisuke Suzuki, MD, Naoki Atsuta, MD, Hirohisa Watanabe, MD, Fumiaki Tanaka, MD, Manabu Doyu, MD, and Gen Sobue, MD

Objective: Spinal and bulbar muscular atrophy (SBMA) is a hereditary motor neuron disease caused by the expansion of a polyglutamine tract in the androgen receptor (AR). The nuclear accumulation of mutant AR is central to the pathogenesis of SBMA. Androgen deprivation with leuprorelin inhibits mutant AR accumulation, resulting in rescue of neuronal dysfunction in a mouse model of SBMA. This study aimed to investigate whether mutant AR accumulation in the scrotal skin is an appropriate biomarker of SBMA. _Methods:_ Immunohistochemistry of both scrotal skin and the spinal cord was performed on five autopsied SBMA cases. Neurological severity and scrotal skin findings were studied in another 13 patients. Five other patients received subcutaneous injections of leuprorelin and underwent scrotal skin biopsy. _Results:_ The degree of mutant AR accumulation in scrotal skin epithelial cells tended to be correlated with that in the spinal motor neurons in autopsy specimens, and it was well correlated with CAG repeat length and inversely correlated with the amyotrophic lateral sclerosis functional scale. Leuprorelin treatment inhibited mutant AR protein accumulation in the scrotal skin of SBMA patients. _Interpretation:_ These observations suggest that scrotal skin biopsy findings are a potent pathogenic marker of SBMA and can be a surrogate end point in therapeutic trials.

Ann Neurol 2006;59:520–526

Spinal and bulbar muscular atrophy (SBMA), also known as Kennedy's disease, is an adult-onset motor neuron disease characterized by muscle atrophy, weakness, contraction fasciculations, and bulbar involvement.[1–4] SBMA exclusively affects men in their 30s or 40s, and disease progression is slow.[1,5] The molecular basis of SBMA is the expansion of a trinucleotide CAG repeat, which encodes a polyglutamine (polyQ) tract, in the androgen receptor (AR) gene.[6] The CAG repeat numbers range from 38 to 62 in SBMA patients, whereas healthy individuals have 10 to 36 CAGs.[6,7] The number of CAGs is correlated with disease severity and is inversely correlated with age of onset,[8,9] as observed in other polyQ-related neurodegenerative diseases including Huntington's disease and several forms of spinocerebellar ataxia.[10]

Histopathologically, lower motor neurons are markedly depleted in the spinal cord and brainstem, and nuclear inclusions (NIs) containing the mutant and truncated AR with expanded polyQ are present in the residual motor neurons, as well as in cells of the scrotal skin and other visceral organs.[3,11,12] Although NIs are a disease-specific pathological marker, they may reflect a cellular protective response against the toxicity of abnormal polyQ-containing protein.[13] In contrast, the therapeutic effect of testosterone deprivation in our SBMA transgenic mouse model suggested that diffuse nuclear accumulation of mutant AR is a cardinal pathogenic process underlying neurological manifestations.[14,15] This hypothesis has also been clearly illustrated by the observation that the extent of diffuse nuclear accumulation of mutant AR, but not NIs, in the motor neurons of the spinal cord was closely related to CAG repeat length in autopsied SBMA cases.[16] Nuclear localization of the mutant protein has now been considered essential for inducing neuronal cell dysfunction and degeneration in the majority of polyQ diseases.[10]

A characteristic clinical feature of SBMA is that the disease occurs in male but not female individuals, even when they are homozygous for the mutation.[17,18] Several studies have clarified that the sex dependency of disease manifestation in SBMA arises from testosterone-dependent nuclear accumulation of mu-

---

From the Department of Neurology, Nagoya University Graduate School of Medicine, Showa-ku, Nagoya, Japan.

Received Sep 1, 2005, and in revised form Oct 4. Accepted for publication Oct 6, 2005.

DOI: 10.1002/ana.20735

Address correspondence to Dr Sobue, Department of Neurology, Nagoya University Graduate School of Medicine, 65 Tsurumai-cho, Showa-ku, Nagoya 466-8550, Japan.
E-mail: sobueg@med.nagoya-u.ac.jp

tant AR.[14,15,19,20] Leuprorelin, a leuteinizing hormone–releasing hormone agonist that reduces testosterone release from the testis and inhibits nuclear accumulation of mutant AR, rescued motor dysfunction in male transgenic mice carrying the full-length human AR with expanded polyQ.[15]

Although data from transgenic mice studies indicated that androgen deprivation from leuprorelin treatment is a potent therapeutic agent for SBMA,[14,15] clinical experience using this drug for SBMA patients is limited.[21] Because long-term clinical trials are needed to establish the efficacy of therapeutics ameliorating disease progression in slowly progressive neurodegenerative diseases such as SBMA, an appropriate biomarker reflecting pathogenic processes of the disease is necessary. The aim of this study was to test the hypothesis that peripheral accumulation of mutant AR in the scrotal skin represents a suitable biomarker of SBMA that can be applicable as a surrogate end point in therapeutic trials.

Patients and Methods

Patients

Twenty-three patients with clinically and genetically confirmed SBMA were examined. Patient characteristics are shown in the Table. Five of the 23 patients underwent autopsy, and both the scrotal skin and the spinal cord were examined; another 13 patients underwent biopsy of the scrotal skin. The remaining five patients were enrolled in a leuprorelin study and also underwent biopsy of the scrotal skin. All patients were hospitalized and underwent follow-up examinations at Nagoya University Hospital (Nagoya, Japan) and its affiliated hospitals.

For each of the 18 patients who underwent biopsy of the scrotal skin, three scrotal skin specimens were made by punch biopsy using a 3mm diameter Dermapunch (Nipro, Tokyo, Japan) under 10ml lidocaine acetate local anesthesia. All patients who underwent biopsy sterilized the wound for several days by themselves and received 4 days of cefaclor (250mg three times a day) antibiotic therapy after the procedure. The 13 patients who underwent biopsy who were not enrolled in the leuprorelin trial were also assessed on the amyotrophic lateral sclerosis functional scale (limb Norris score), as described previously.[22]

Five other male subjects (age, 60–74 years; mean, 67.3 years) who died of nonneurological diseases served as control subjects. The Nagoya University Hospital Institutional Review Board approved the collection of data and specimens, and all patients gave their written, informed consent to participate.

Leuprorelin Administration

Five patients received subcutaneous injections of 3.75mg leuprorelin once every 4 weeks. The patients, aged 43 to 68 years, were capable of walking with or without a cane and expressed no desire to father a child. They were observed for 6 months (24 weeks), and scrotal skin biopsies were taken from each patient at 0, 4, and 12 weeks after initial leuprorelin administration. Serum creatine kinase (CK) was determined by ultraviolet measurement using hexokinase and glucose-6-phosphate. Serum testosterone levels were measured by radioimmunoassay using the DPC total testosterone kit (Diagnostic Products Corporation, Los Angeles, CA).

Immunohistochemical Detection of the Mutant Androgen Receptor in the Scrotal Skin and Spinal Cord

Immunohistochemistry of scrotal skin specimens and the spinal cord were conducted as described previously.[16] In brief, we prepared 5μm-thick, formalin-fixed, paraffin-embedded sections of scrotal skin and spinal cord from SBMA patients. Sections were deparaffinized and rehydrated through a graded series of alcohol-water solutions. For the mutant AR immunohistochemical study, sections were pretreated with immersion in 98% formic acid for 5 minutes, and then with microwave oven heating for 15 minutes in 10mM citrate buffer at pH 6.0. Sections were incubated with a mouse anti-expanded polyQ antibody (1:20,000; 1C2; Chemicon, Temecula, CA)[23] to evaluate the nuclear accumulation of mutant AR.[14–16] Immune complexes were visualized using the Envision-plus kit (Dako, Glostrup, Denmark). Sections were counterstained with Mayer's hematoxylin. For electron microscopic immunohistochemistry, the sections were processed

Table. Patient Characteristics

Characteristics	Autopsy Study (N = 5)	Biopsy Alone Study (N = 13)	Leuprorelin + Biopsy Study (N = 5)
Age (mean ± SD), yr	64.8 ± 10.8	54.8 ± 9.6	50.2 ± 10.8
Duration of weakness (mean ± SD), yr	38.4 ± 14.7	11.0 ± 7.4	8.8 ± 4.9
(CAG)n (mean ± SD)	47.4 ± 4.9	48.2 ± 3.0	49.2 ± 4.9
ADL (cane/independent ratio)	NA	4/9	2/3
Limb Norris score (mean ± SD)	NA	53.4 ± 6.9	52.0 ± 6.8
Norris bulbar score (mean ± SD)	NA	32.2 ± 3.4	32.8 ± 6.2
ALSFRS-R (Japanese edition) (mean ± SD)	NA	40.3 ± 3.2	39.2 ± 3.8
Cause of death	Pneumonia (n = 4); Lung cancer (n = 1)	NA	NA

The amyotrophic lateral sclerosis functional rating scale-revised.
SD = standard deviation; (CAG)n = number of expanded CAG repeats in the SBMA allele; NA = not applicable; ADL = activities of daily living.

as described for light microscopic immunohistochemistry, and then fixed with 2% osmium tetroxide in 0.1M phosphate buffer at pH 7.4, dehydrated in graded alcohol-water solutions, and embedded in epoxy resin. Ultrathin sections were cut for observation under an electron microscope (H-7100; Hitachi High-Technologies Corporation, Tokyo, Japan).

Quantification of Cell Population with Diffuse Nuclear Staining

For quantitative assessment of scrotal skin cells, the frequency of diffuse nuclear staining was calculated from counts of more than 500 nuclei in 5 randomly selected fields of each section photographed at 400× magnification (BX51TF; Olympus, Tokyo, Japan). To assess the nuclear accumulation of mutant AR in spinal cord motor neurons, we prepared at least 100 transverse sections each from the cervical, thoracic, and lumber spinal cord for anti-expanded polyQ antibody staining with 1C2. The numbers of 1C2-positive cells in the ventral horn on both the right and left sides were counted on every 10th section under the light microscope with a computer-assisted image analyzer (BX51TF; Olympus), as described previously.[16,24] Populations of 1C2-positive cells were expressed as percentages of the total skin cell or neuronal count.

Statistical Analysis

We analyzed the data by Pearson's coefficient, Spearman's rank correlation, and Student's paired t test as appropriate using StatView software (version 5; Hulinks, Tokyo, Japan) and considering p values less than 0.05 to be indicative of significance.

Results

Mutant Androgen Receptor Nuclear Accumulation in the Scrotal Skin and Spinal Motor Neuron

In the five autopsied cases, mutant AR nuclear accumulations were clearly visualized with anti-expanded polyQ immunostaining with 1C2 in the scrotal skin and spinal cord specimens (Fig 1A). Pathological accumulation of mutant AR was distributed in all layers of the epithelium. Diffuse nuclear accumulations were predominantly observed, and the occurrence of NIs was less frequent. This was also the case in the spinal cord specimens. Electron microscopic immunohistochemistry with the 1C2 antibody demonstrated granular dense and amorphous aggregates corresponding to diffuse nuclear staining in both spinal motor neurons and epithelial cells of scrotal skin (see Figs 1B, C). Filamentous structures such as those reported in Huntington's disease,[25] dentatorubal-pallidoluysian atrophy (DRPLA),[26] and Machado–Joseph disease[27] were not seen. No diffuse nuclear staining was seen in the control subjects. The extent of mutant AR accumulation in the scrotal skin epithelial cells showed a tendency to correlate with that in the anterior horn cells ($r = 0.84$; $p = 0.08$; see Fig 1D). Mutant AR accumulation was remarkable in both the spinal motor neurons and the scrotal skin of Patient 1, but was far less remarkable in Patient 2 (see Figs 1A, D).

Correlations of the Mutant Androgen Receptor Accumulation in the Scrotal Skin to CAG Repeat Length and Amyotrophic Lateral Sclerosis Score

Mutant AR nuclear accumulations in scrotal skin biopsies from the 13 SBMA patients who did not receive leuprorelin were assessed by 1C2 antibody staining of expanded PolyQ. The 1C2-positive cell population in the scrotal skin biopsies was significantly correlated with CAG repeat length ($r = 0.61$; $p = 0.03$; Fig 2A) and was inversely correlated with the functional scale assessed by the Norris score on limbs ($r = -0.63$; $p = 0.02$; see Fig 2B).

Leuprorelin Treatment Depletes Mutant Androgen Receptor Accumulation in the Scrotal Skin

In all five patients in which leuprorelin was administered (see the Table), both the intensity and the frequency of diffuse nuclear 1C2 staining in the scrotal epithelial cells was decreased after the first 4 weeks of administration compared with the preadministration values, and this effect was markedly enhanced after 12 weeks of treatment (Figs 3A, B). Quantitative analysis demonstrated a significant decrease in the frequency of 1C2-positive cells both 4 and 12 weeks after the initiation of leuprorelin treatment ($p < 0.01$) (see Fig 3C). Serum testosterone levels decreased to the castration level after 1 to 2 months of treatment (see Fig 3D), and serum CK values were also significantly decreased in all patients (see Fig 3D).

None of the patients showed the hot flush or obesity often reported in leuprorelin trials for prostate cancer. Although a loss of sexual function including erectile disorder was observed in all patients, no patients experienced depression. No marked exacerbations were observed in total cholesterol, triglyceride, fasting blood sugar, or HbA1c (data not shown). We could not find significant motor function changes assessed by amyotrophic lateral sclerosis functional scores in 24 weeks, but three of the five enrolled patients expressed apparent subjective improvement.

Discussion

This study demonstrated that scrotal skin biopsy with anti-expanded polyQ staining is a strong candidate for an appropriate biomarker with which to monitor SBMA pathogenic processes. Previous studies showed that the severity and progression of motor dysfunction and abatement of abnormalities in mice that were castrated or given leuprorelin paralleled the extent of diffuse nuclear mutant AR accumulation in their spinal motor neurons.[14,15] Furthermore, we demonstrated previously a significant, close correlation between the length of CAG repeat expansion and frequency of dif-

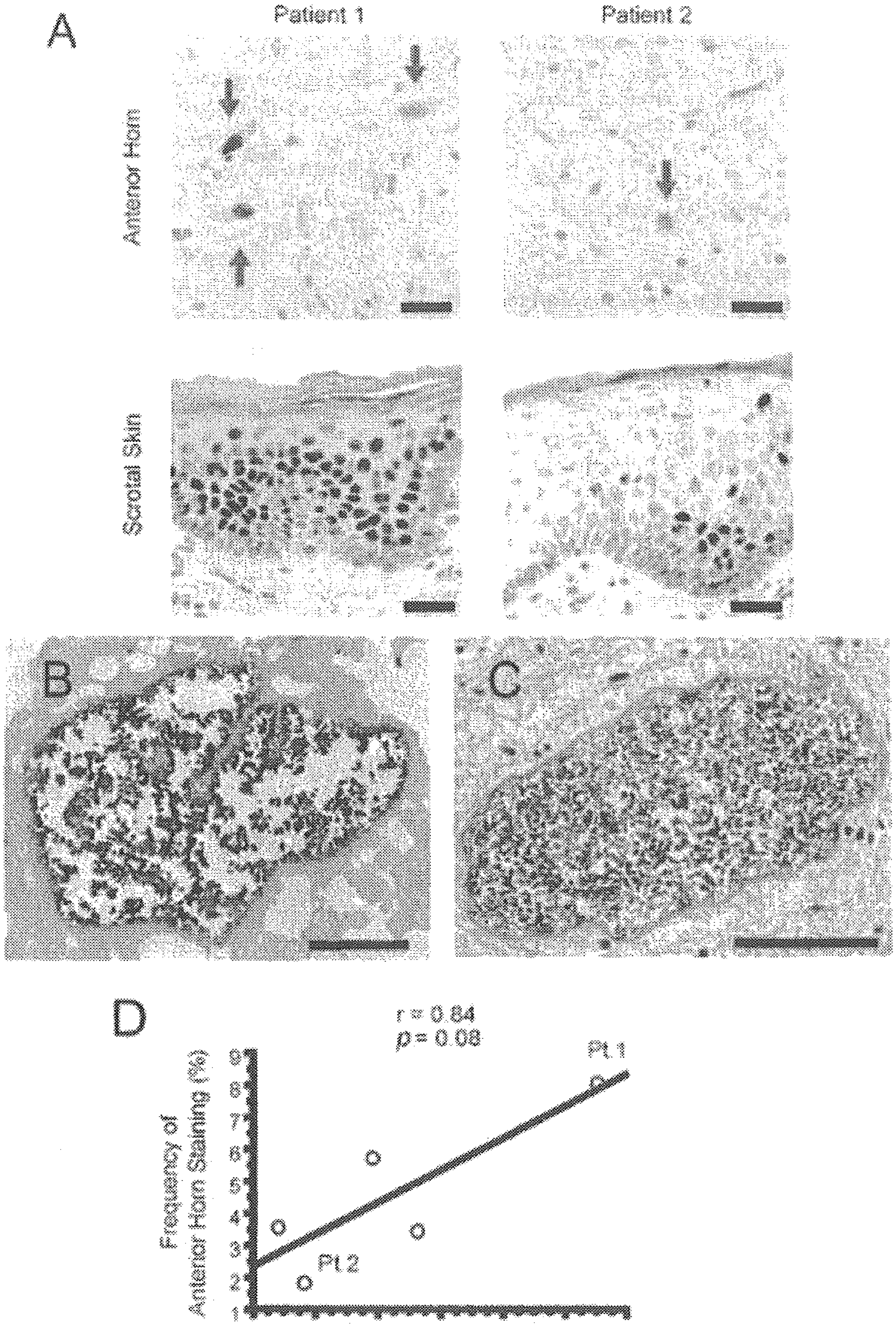

Fig 1. Mutant androgen receptor (AR) nuclear accumulation in scrotal skin and spinal motor neurons. (A) Mutant AR accumulation was remarkable in both spinal motor neurons (arrows) and scrotal skin of Patient 1, but was less remarkable in both motor neurons (arrows) and skin in Patient 2. Bar = 30μm. (B, C) Electron microscopic immunohistochemistry for 1C2 demonstrated granular dense and amorphous aggregates corresponding to diffuse nuclear staining in both spinal motor neurons and epithelial cells of scrotal skin. Bar =3μm. (D) The extent of mutant AR accumulation in scrotal skin epithelial cells showed a tendency to correlate with that in anterior horn cells. Circles (Pt. 1, Pt. 2) correspond to Patient 1 and 2 in Fig 1A.

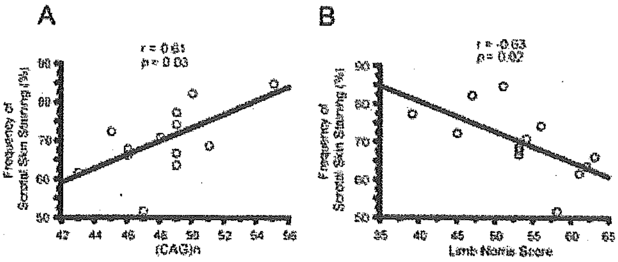

Fig 2. Correlation of the frequency of scrotal skin staining to CAG repeats and limb Norris score. The frequency of 1C2-positive cells in the scrotal skin biopsies correlated significantly with (A) CAG repeat length and (B) inversely correlated with the amyotrophic lateral sclerosis functional scale assessed by the Norris score on limbs. (CAG)n = number of expanded CAG repeats in the spinal and bulbar muscular atrophy allele.

fuse nuclear mutant AR accumulation, but not that of NIs, in the spinal cord.[16] Accordingly, neuronal dysfunction is likely to be caused by diffuse nuclear accumulation of mutant AR in the affected tissues. In this study, the extent of mutant AR nuclear accumulation in scrotal skin cells paralleled that in the anterior horn cells in autopsied cases. Electron microscopic immunohistochemistry for 1C2 anti-expanded PolyQ demonstrated granular dense and amorphous aggregates corresponding to diffuse nuclear staining in both spinal motor neurons and epithelial cells of scrotal skin. Furthermore, the fine structure of the aggregates in spinal motor neurons and epithelial cells was quite similar. Biopsy analyses in this study also suggested that scrotal skin findings were correlated with the motor functional scores of SBMA patients.

Our findings suggest that nuclear mutant AR assessed by 1C2 immunostaining in the scrotal skin is a practical procedure to estimate the severity of SBMA pathogenesis in the nervous system. In support of this view, decreases in mutant AR accumulation in the motor neurons paralleled that in nonneuronal cells in the androgen deprivation therapy tested in the mouse model of SBMA. In addition, leuprorelin treatment markedly reduced serum testosterone levels, as well as nuclear accumulation of mutant AR in the scrotal skin, suggesting that medical castration with leuprorelin intervenes in the pathogenic process of human SBMA, as demonstrated in the animal study. Moreover, serum CK levels were significantly decreased in this leuprorelin study. Because high CK values are common in SBMA patients and histopathological examinations have shown myogenic changes together with neurogenic findings in this disease,[1,3] presumably, a decrease in CK values with leuprorelin treatment implies muscular protection. Serum CK levels, however, did not significantly correlate with the Norris score on limbs or with scrotal skin biopsy findings in our cross-sectional study.

As defined by the Biomarkers Definitions Working Group, a disease biomarker should be objectively measurable and evaluated as an indicator of pathogenic processes or pharmacological responses to a therapeutic intervention.[28] Based on the observations described earlier, 1C2-stained mutant AR accumulation in the biopsied scrotal skin is likely to be a potent biomarker reflecting pathogenic processes of SBMA. Particularly, the correlation of the extent of mutant AR nuclear accumulation in the spinal motor neurons with that in scrotal skin biopsies in the autopsied cases suggests that findings in the scrotal skin can predict pathogenic processes in the motor neurons.

Although its precise natural history has not been evaluated, SBMA is a slowly progressive disease.[1,5] Thus, extremely long-term clinical trials are necessary to assess whether certain drugs can alter the natural disease progression by targeting clinical end points such as occurrence of aspiration pneumonia or becoming wheelchair bound. Suitable surrogate end points, which reflect the pathogenesis and severity of SBMA, are substantial to assess the therapeutic efficacy in drug trials. Although it is not practical to obtain biopsy specimens from the central nervous system (CNS), a punch biopsy of the scrotal skin enables a safe and accessible examination for patients.

It has also been suggested that reliance on surrogate end points can be misleading because they may not accurately predict the actual effects that treatments have on the health of a patient, as was seen with the CD4 counts in human immunodeficiency virus trials, the bone mineral density in osteoporosis trials, and others.[29] However, several factors have been suggested to consider the decision to rely on a surrogate.[30] In SBMA, mutant AR accumulation assessed by scrotal skin biopsy can be a candidate for a surrogate end point in light of several pieces of evidence. First, a credible SBMA animal model demonstrated dramatic functional motor recovery in response to testosterone deprivation therapy that depleted mutant AR accumulation in the central nervous system, as well as in nonneuronal tissues.[14,15] Second, the degree of diffuse nuclear accumulation of mutant AR in both the CNS and scrotal skin correlates well with CAG repeat length and disease severity, indicating that it is a natural phenomenon of and reflects the underlying pathology of the disease. Third, autopsy studies show that levels of nuclear AR accumulation in the scrotal skin are correlated with those in the CNS. Moreover, levels of nuclear translocated mutant AR in the scrotal skin decreased significantly in response to drug therapy that has been shown to deplete such accumulations in the CNS of SBMA mice, to significantly rescue motor dysfunction in these mice, and to partially stabilize neurological symptoms in one reported case of human SBMA.[21]

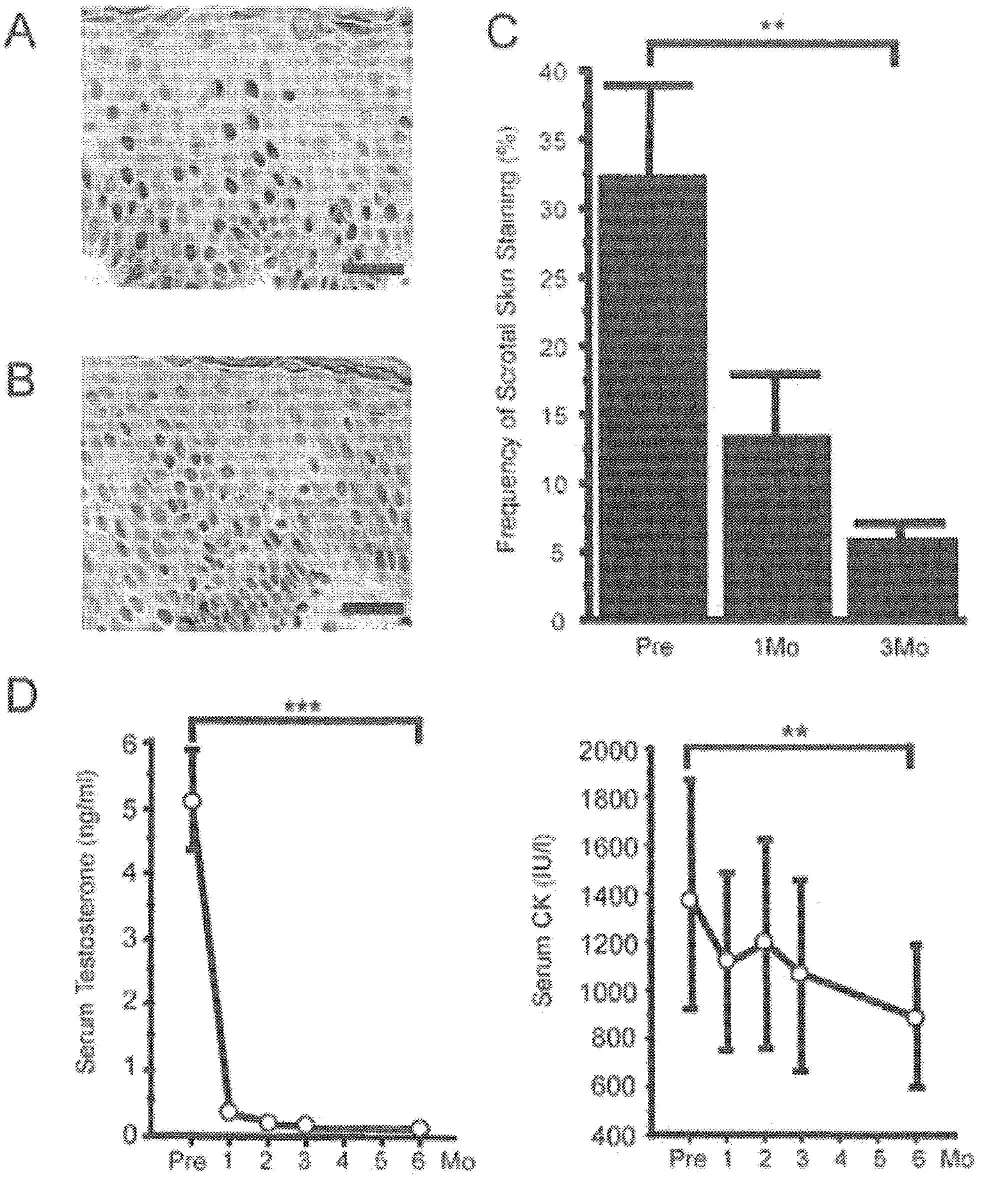

Fig 3. Effects of leuprorelin on mutant androgen receptor (AR) accumulation in scrotal skin, serum testosterone, and creatine kinase (CK). (A) Scrotal skin shows intense and frequent staining for anti-polyglutamine antibody in the nucleus before therapy. (B) Twelve weeks after therapy, both intensity and frequency of nuclear staining markedly decreased. Bar = 30μm. (C) Quantitative analysis of immunohistochemistry demonstrated a significant decrease in the number of positively stained nuclei. (D) Serum testosterone and CK decreased significantly in 6 months. Frequency of staining was calculated from counts of more than 500 nuclei in randomly selected areas and was expressed as mean ± standard deviation for 5 patients. $^{**}p < 0.01$; $^{***}p < 0.0001$.

Although our results were obtained from a small sample, nuclear accumulation of mutant AR in the scrotal skin appears to be a potent pathogenic biomarker of SBMA. A correlation between decline in validated clinical scales and nuclear mutant AR accumulations must be demonstrated in a longitudinal study to verify this histopathological feature as a biomarker for clinical severity. Similarly, validation of the scrotal skin biopsy findings as a surrogate end point in clinical trials will require a longitudinal study verifying that suppression of nuclear staining correlates with improvement on a validated clinical scale and the true clinical outcome events such as the need for a wheelchair, the presence of aspiration pneumonia, or death.

This work was supported by grants from the Ministry of Education, Culture, Sports, Science and Technology, Japan (17204032, G. S., M. D., F. T.); the Ministry of Health, Labor and Welfare, Japan (H-15-Kokoro-020, G. S., M. D.); and the Center for Clinical Trials, Japan Medical Association (G.S.).

We thank Dr N. Hishikawa for technical assistance.

References

1. Kennedy WR, Alter M, Sung JH. Progressive proximal spinal and bulbar muscular atrophy of late onset: a sex-linked recessive trait. Neurology 1968;18:671–680.
2. Sperfeld AD, Karitzky J, Brummer D, et al. X-linked bulbospinal neuropathy: Kennedy disease. Arch Neurol 2002;59:1921–1926.
3. Sobue G, Hashizume Y, Mukai E, et al. X-linked recessive bulbospinal neuronopathy: a clinicopathological study. Brain 1989;112:209–232.
4. Katsuno M, Adachi H, Tanaka F, et al. Spinal and bulbar muscular atrophy (SBMA): ligand-dependent pathogenesis and therapeutic perspective. J Mol Med 2004;82:298–307.
5. Sobue G, Adachi H, Katsuno M. Spinal and bulbar muscular atrophy (SBMA). In: Dickinson D, ed. Neurodegeneration: the molecular pathology of dementia and movement disorders. Basel: INS Neuropathology, 2003:275–279.
6. La Spada AR, Wilson EM, Lubahn DB, et al. Androgen receptor gene mutations in X-linked spinal and bulbar muscular atrophy. Nature 1991;352:77–79.
7. Tanaka F, Doyu M, Ito Y, et al. Founder effect in spinal and bulbar muscular atrophy (SBMA). Hum Mol Genet 1996;5:1253–1257.
8. Doyu M, Sobue G, Mukai E, et al. Severity of X-linked recessive bulbospinal neuronopathy correlates with size of the tandem CAG repeat in androgen receptor gene. Ann Neurol 1992;32:707–710.
9. Shimada N, Sobue G, Doyu M, et al. X-linked recessive bulbospinal neuronopathy: clinical phenotypes and CAG repeat size in androgen receptor gene. Muscle Nerve 1995;18:1378–1384.
10. Zoghbi HY, Orr HT. Glutamine repeats and neurodegeneration. Annu Rev Neurosci 2000;23:217–247.
11. Li M, Miwa S, Kobayashi Y, et al. Nuclear inclusions of the androgen receptor protein in spinal and bulbar muscular atrophy. Ann Neurol 1998;44:249–254.
12. Li M, Nakagomi Y, Kobayashi Y, et al. Nonneural nuclear inclusions of androgen receptor protein in spinal and bulbar muscular atrophy. Am J Pathol 1998;153:695–701.
13. Arrasate M, Mitra S, Schweitzer ES, et al. Inclusion body formation reduces levels of mutant huntingtin and the risk of neuronal death. Nature 2004;431:805–810.
14. Katsuno M, Adachi H, Kume A, et al. Testosterone reduction prevents phenotypic expression in a transgenic mouse model of spinal and bulbar muscular atrophy. Neuron 2002;35:843–854.
15. Katsuno M, Adachi H, Doyu M, et al. Leuprorelin rescues polyglutamine-dependent phenotypes in a transgenic mouse model of spinal and bulbar muscular atrophy. Nat Med 2003;9:768–773.
16. Adachi H, Katsuno M, Minamiyama M, et al. Widespread nuclear and cytoplasmic accumulation of mutant androgen receptor in SBMA patients. Brain 2005;128:659–670.
17. Sobue G, Doyu M, Kachi T, et al. Subclinical phenotypic expressions in heterozygous females of X-linked recessive bulbospinal neuronopathy. J Neurol Sci 1993;117:74–78.
18. Schmidt BJ, Greenberg CR, Allingham-Hawkins DJ, Spriggs EL. Expression of X-linked bulbospinal muscular atrophy (Kennedy disease) in two homozygous women. Neurology 2002;59:770–772.
19. Takeyama K, Ito S, Yamamoto A, et al. Androgen-dependent neurodegeneration by polyglutamine-expanded human androgen receptor in Drosophila. Neuron 2002;35:855–864.
20. Chevalier-Larsen ES, O'Brien CJ, Wang H, et al. Castration restores function and neurofilament alterations of aged symptomatic males in a transgenic mouse model of spinal and bulbar muscular atrophy. J Neurosci 2004;24:4778–4786.
21. Shimohata T, Kimura T, Nishizawa M, et al. Five year follow up of a patient with spinal and bulbar muscular atrophy treated with leuprorelin. J Neurol Neurosurg Psychiatry 2004;75:1206–1207.
22. Norris FH Jr, Calanchini PR, Fallat RJ, et al. The administration of guanidine in amyotrophic lateral sclerosis. Neurology 1974;24:721–728.
23. Trottier Y, Lutz Y, Stevanin G, et al. Polyglutamine expansion as a pathological epitope in Huntington's disease and four dominant cerebellar ataxias. Nature 1995;378:403–406.
24. Terao S, Sobue G, Hashizume Y, et al. Age-related changes in human spinal ventral horn cells with special reference to the loss of small neurons in the intermediate zone: a quantitative analysis. Acta Neuropathol (Berl) 1996;92:109–114.
25. DiFiglia M, Sapp E, Chase KO, et al. Aggregation of huntingtin in neuronal intranuclear inclusions and dystrophic neurites in brain. Science 1997;277:1990–1993.
26. Hayashi Y, Kakita A, Yamada M, et al. Hereditary dentatorubral-pallidoluysian atrophy: ubiquitinated filamentous inclusions in the cerebellar dentate nucleus neurons. Acta Neuropathol (Berl) 1998;95:479–482.
27. Paulson HL, Perez MK, Trottier Y, et al. Intranuclear inclusions of expanded polyglutamine protein in spinocerebellar ataxia type 3. Neuron 1997;19:333–344.
28. Biomarkers Definitions Working Group. Biomarkers and surrogate endpoints: preferred definitions and conceptual framework. Clin Pharmacol Ther 2001;69:89–95.
29. Fleming TR, DeMets DL. Surrogate end points in clinical trials: are we being misled? Ann Intern Med 1996;125:605–613.
30. Temple R. Are surrogate markers adequate to assess cardiovascular disease drugs? JAMA 1999;282:790–795.

Wiley InterScience
DISCOVER SOMETHING GREAT

Journal of Neuroscience Research 83:119–133 (2006)

Disease Progression of Human SOD1 (G93A) Transgenic ALS Model Rats

Arifumi Matsumoto,[1,3,6] Yohei Okada,[1,4,6] Masanori Nakamichi,[5] Masaya Nakamura,[2] Yoshiaki Toyama,[2] Gen Sobue,[4] Makiko Nagai,[3] Masashi Aoki,[3] Yasuto Itoyama,[3] and Hideyuki Okano[1,6]*

[1]Department of Physiology, Keio University School of Medicine, Tokyo, Japan
[2]Department of Orthopaedic Surgery, Keio University School of Medicine, Tokyo, Japan
[3]Department of Neurology, Tohoku University Graduate School of Medicine, Sendai, Japan
[4]Department of Neurology, Nagoya University Graduate School of Medicine, Nagoya, Japan
[5]Takeda Chemical Industries, Ltd., Osaka, Japan
[6]Core Research for Evolutional Science and Technology (CREST), Japan Science and Technology Agency (JST), Saitama, Japan

The recent development of a rat model of amyotrophic lateral sclerosis (ALS) in which the rats harbor a mutated human SOD1 (G93A) gene has greatly expanded the range of potential experiments, because the rats' large size permits biochemical analyses and therapeutic trials, such as the intrathecal injection of new drugs and stem cell transplantation. The precise nature of this disease model remains unclear. We described three disease phenotypes: the forelimb-, hindlimb-, and general-types. We also established a simple, non-invasive, and objective evaluation system using the body weight, inclined plane test, cage activity, automated motion analysis system (SCANET), and righting reflex. Moreover, we created a novel scale, the Motor score, which can be used with any phenotype and does not require special apparatuses. With these methods, we uniformly and quantitatively assessed the onset, progression, and disease duration, and clearly presented the variable clinical course of this model; disease progression after the onset was more aggressive in the forelimb-type than in the hindlimb-type. More importantly, the disease stages defined by our evaluation system correlated well with the loss of spinal motor neurons. In particular, the onset of muscle weakness coincided with the loss of approximately 50% of spinal motor neurons. This study should provide a valuable tool for future experiments to test potential ALS therapies.

Key words: amyotrophic lateral sclerosis; evaluation system; behavioral analyses; phenotype; variability

Amyotrophic lateral sclerosis (ALS) is a fatal neurodegenerative disorder that mainly affects the upper and lower motor neurons (de Belleroche et al., 1995). It is characterized by progressive muscle weakness, amyotrophy, and death from respiratory paralysis, usually within 3–5 years of onset (Brown 1995). Although most cases of ALS are sporadic (SALS), approximately 10% are familial (FALS) (Mulder et al., 1986). Moreover, 20–25% of FALS cases are due to mutations in the gene encoding copper-zinc superoxide dismutase (SOD1) (Deng et al., 1993; Rosen et al., 1993). More than 100 different mutations in the SOD1 gene have been identified in FALS so far.

Until recently, animal models of FALS have been various transgenic mice that express a mutant human SOD1 (hSOD1) gene. Of these, a transgenic mouse carrying the G93A (Gly-93 → Ala) mutant hSOD1 gene was the first described (Gurney et al., 1994) and is used all over the world because this model closely recapitulates the clinical and histopathological features of the human disease. To evaluate the therapeutic effects of potential ALS treatments in this animal, many motor-related behavioral tasks are used (Chiu et al., 1995; Barneoud et al., 1997; Garbuzova-Davis et al., 2002; Sun et al., 2002; Wang et al., 2002; Inoue et al., 2003; Kaspar et al., 2003; Weydt et al., 2003; Azzouz et al., 2004). However, transgenic mice have innate limitations for some types of experiments because of their small size.

Recently, transgenic rat models of ALS, which harbor the hSOD1 gene containing the H46R (His-46 → Arg) or G93A mutation were generated (Nagai et al., 2001). The larger size of these rat models makes certain experiments easier, such as biochemical analyses that require large amounts of sample, intrathecal administration

Contract grant sponsor: Core Research for Evolutional Science and Technology (CREST), Japan Science and Technology Agency (JST); Contract grant sponsor: Japanese Ministry of Health, Labour and Welfare; Contract grant sponsor: Japanese Ministry of Education, Culture, Sports, Science and Technology.

*Correspondence to: Hideyuki Okano, Department of Physiology, School of Medicine, Keio University, 35 Shinanomachi, Shinjuku-ku, Tokyo, 160-8582, Japan. E-mail: hidokano@sc.itc.keio.ac.jp

Received 22 August 2005; Revised 29 September 2005; Accepted 30 September 2005

DOI: 10.1002/jnr.20708

of drugs, and, especially, therapeutic trials, including the transplantation of neural stem cells into the spinal cord. The hSOD1 (G93A) transgenic rats typically present weakness in one hindlimb first. Later, weakness progresses to the other hindlimb and to the forelimbs. Finally, the rats usually become unable to eat or drink, and eventually die. Only subjective and ambiguous analyses were made with regard to the clinical progression of this ALS animal model and objective criteria for evaluating the efficacy of these new treatments have not been determined. For these reasons, we assessed the disease progression quantitatively using five different measures (body weight, inclined plane test, cage activity, SCANET, and righting reflex) and established an easy, noninvasive, and objective evaluation system that is sensitive to small but important abnormalities in the hSOD1 (G93A) transgenic rats. In addition, we created a novel scale, the Motor score, to assess disease progression in the transgenic rats without using special apparatuses. We also examined the validity of these measures as assessment tools for the pathology by investigating the number of spinal motor neurons remaining at the disease stages defined by each measure.

MATERIALS AND METHODS

Transgenic Rats

All animal experiments were conducted according to the Guidelines for the Care and Use of Laboratory Animals of Keio University School of Medicine. We used hSOD1 (G93A) transgenic male rats (Nagai et al., 2001) from our colony and their age- and gender-matched wild-type littermates as controls. Rats were housed in a specific pathogen-free animal facility at a room temperature of 23 ± 1°C under a 12-hr light-dark cycle (light on at 08:00). Food (solid feed CE-2, 30kGy; CLEA Japan, Inc.) and water were available ad lib. Transgenic rats were bred and maintained as hemizygotes by mating transgenic males with wild-type females. Transgenic progeny were identified by detecting the exogenous hSOD1 transgene, by amplification of pup tail DNA extracted at 20 days of age by polymerase chain reaction (PCR). The primers and cycling conditions were described previously (Nagai et al., 2001).

Exploration of Assessment Tools to Measure Disease Progression in the hSOD1 (G93A) Transgenic Rats

We evaluated the usefulness of four different measures to assess disease progression in the transgenic rats. All tests were carried out between 12:00–16:00 and in a double-blind fashion.

Body weight. Animals ($n = 9$ for each genotype) were weighed weekly after 30 days of age with an electronic scale. To avoid overlooking the beginning of weight loss, the animals were weighed every second or third day after 90 days of age, the age at which motor neurons are reported to be lost in the lumbar spinal cord (Nagai et al., 2001).

Inclined plane. This test was initially established mainly to assess the total strength of the forelimbs and hindlimbs in a model of spinal cord injury (Rivlin and Tator, 1977). Briefly, rats were placed laterally against the long axis of the inclined plane, and the maximum angle at which they could maintain their position on the plane for 5 sec was measured. To assess the strength of both sides of limbs equally, animals were placed on the inclined plane with the right side of the body to the downhill side of the incline, and then with the left side of the body facing downhill. For each rat, the test was carried out three times for each side, and the mean value of the angles obtained for the right side was compared to that obtained for the left. The lower mean value was recorded as the angle for that rat. Animals ($n = 9$ for each genotype) were tested weekly after 70 days of age and every second to third day after 100 days of age.

Cage activity. Animals ($n = 8$ for each genotype) were housed individually and monitored every day for all 24 hr (except for the days the cages were changed) after they were 70 days old. Spontaneous locomotor activity in the home cage (345 × 403 × 177 mm) was recorded by an activity-monitoring system (NS-AS01; Neuroscience, Inc., Tokyo, Japan) as described previously (Ohki-Hamazaki et al., 1999). The sensor detects the movement of animals using the released infrared radiation associated with their body temperature. The data were analyzed by the DAS-008 software (Neuroscience, Inc., Tokyo, Japan). To eliminate data variability owing to differences in the baseline movement of each rat, the baseline value was calculated as the mean of movement from 70–90 days of age, during which all rats were considered to move normally. We analyzed the data at each time point as the percentage of the baseline value in defining disease onset with this test.

SCANET. For short-term activity, 10 min of spontaneous activity was measured with the automated motion analysis system SCANET MV-10 (Toyo Sangyo Co., Ltd., Toyama, Japan) (Mikami et al., 2002). Animals ($n = 4$ for each genotype) were tested weekly after 30 days of age and every second or third day after 100 days of age. Each rat was individually placed in the SCANET cage for 10 min. Three parameters were measured: small horizontal movements of 12 mm or more (Move 1; M1), large horizontal movements of 60 mm or more (Move 2; M2), and the frequency of vertical movements caused by rearing (RG). To distinguish RG movements from incomplete standing actions, the upper sensor frame was adjusted to 13 cm above the lower sensor frame.

Righting reflex. All affected animals were tested for the ability to right themselves within 30 sec of being turned on either side (righting reflex) (Gale et al., 1985). Failure was seen when animals reached the end-stage of disease (Howland et al., 2002), and was regarded as a generalized loss of motor activity. We used this time point, which we call "end-stage," as "death" rather than the actual death of the animal, to exclude the influence of poor food intake and respiratory muscle paralysis on the survival period. All end-stage animals were sacrificed after being deeply anesthetized.

All statistical analyses were carried out with the two-tailed unpaired Student's t-test. A P-value of <0.05 was considered statistically significant.

Motor Score

To establish our own scoring system for motor function, which could be uniformly applicable to any disease phenotype of this rat model, we examined the common clinical findings

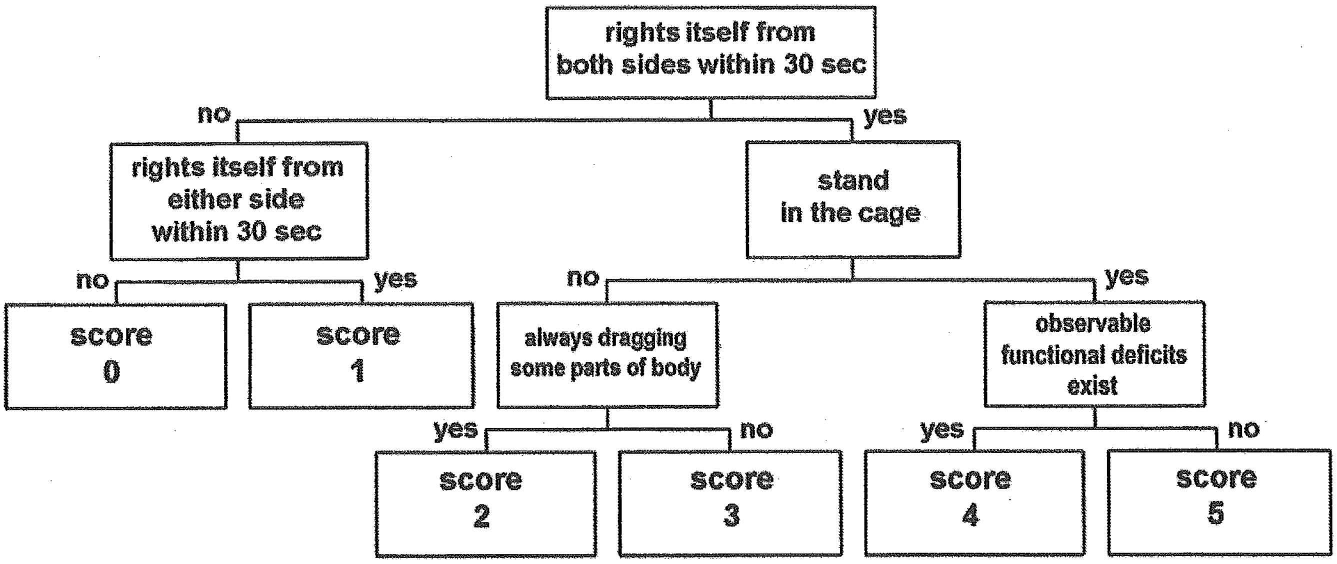

Fig. 1. Chart of Motor score assessment. The degree of motor dysfunction can be assessed by the Motor score as shown in this chart. This scoring system is meant to be used after disease onset, which can be prospectively diagnosed by the inclined plane test (muscle weakness onset). A score of 4 means the same condition as seen for subjective onset (SO). Rats with a score of 5 seem almost as normal as wild-type rats. The detailed testing procedure for the Motor score is described in the text.

of the transgenic rats in detail and assessed their motor functions ($n = 20$). We focused on the following tests: the righting reflex, the ability to stand in the cage, the extent of dragging their bodies when moving, and the existence of observable functional deficits. We evaluated these items sequentially along with the disease progression and classified the rats into six groups by giving them scores between 0 and 5. The scoring chart (Motor score) is shown in Figure 1.

When disease onset in the rats was diagnosed by their scoring <70° on the inclined plane test (muscle weakness onset), the affected rats were tested for righting reflex. If they were unable to right themselves from either side, they were given a score of 0. If they could right themselves from only one side but not the other, they were given a score of 1.

Rats that could right themselves from both sides were examined for the ability to stand in the cage as follows: Rats were observed in the home cage for 1 min to see if they would stand spontaneously (Step 1). When they moved little in the home cage or showed no tendency to stand during Step 1, they were stimulated by being transferred to another cage (Step 2), and then by being returned to their home cage again (Step 3); the transfers were done to activate exploration motivation. During Step 3, the rats were further stimulated by lightly knocking the cage to intensify the motivation to explore. Each step was carried out for 1 min and the test was stopped when the rat stood once. Rats were judged as "unable to stand" if they did not stand, even after all three steps.

Rats that did not stand were subjected to the next test in the open field, where the extent to which they dragged their bodies when moving was assessed. Those who always dragged and could not lift some parts of their bodies except for scrotums and tails at any time were given a score of 2. If they could lift their dragging parts off the ground for even a moment, they were given a score of 3. The phenotype of dragging the forelimbs was different from that of dragging the hindlimbs. As disease progressed, "forelimb-type" rats first began to touch the tips of their noses on the ground, and then began to drag their head and upper trunk as they moved backward with their hindlimbs. "Hindlimb-type" rats dragged their lower trunk and moved forward with their forelimbs.

Finally, rats that had no abnormality in the above-mentioned assessments were examined in detail to see whether they had any observable functional deficits such as paralysis of the limbs or symptoms of general muscle weakness (e.g., walking with a limp, sluggish movement) in the open field. This condition could be judged subjectively and was defined as subjective onset. Rats with any of these symptoms were given a score of 4; otherwise they were given a score of 5.

Because the scores were based on subjective judgment, they might vary depending on the examiner. To examine inter-rater variability, three transgenic rats of different clinical types were examined according to the method described above, recorded on video tape, and subsequently scored by five observers from different backgrounds (Table I). The scores classified by the five observers were statistically analyzed for inter-rater agreement using Cohen's κ statistics (Table II). Kappa values can range from 0 (no agreement) to 1.00 (perfect agreement), and can be interpreted as poor (<0.00), slight (0.00–0.20), fair (0.21–0.40), moderate (0.41–0.60), substantial (0.61–0.80), and almost perfect (0.81–1.00) (Landis and Koch, 1977). The scores for the three transgenic rats were, on the whole, quite consistent among the five observers, suggesting that the Motor score can be used as an objective method for assessing disease progression.

TABLE I. Motor Score of Transgenic Rats Assessed by Five Different Observers

		Days after onset (days)								
Transgenic rat	Observer	0	1	2	3	4	5	6	7	8
#1407 Eventual hindlimb type										
	A	5	4	4		2	2	1	0	
	B	4	4	4		2	2	1	0	
	C	4	4	4		2	2	1	0	
	D	4	4	4		2	2	1	0	
	E	4	4	4		2	2	1	0	
	Mean	4.2	4	4		2	2	1	0	
#1470 Pure hindlimb type										
	A	5		4	4	2	2	2	2	0
	B	5		4	3	3	2	2	2	0
	C	5		4	3	2	2	2	2	0
	D	4		4	4	2	2	2	2	0
	E	4		4	3	2	2	2	2	0
	Mean	4.6		4	3.4	2.2	2	2	2	0
#1449 Pure forelimb type										
	A	4	3	3	3		2	1	1	0
	B	4	3	3	3		2	1	1	0
	C	3	3	3	3		2	1	1	0
	D	3	3	3	3		2	1	1	0
	E	4	3	2	2		2	1	1	0
	Mean	3.6	3	2.8	2.8		2	1	1	0

TABLE II. The kappa Statistics for Inter-Rater Agreement of Motor Score

	Transgenic rat (clinical type)		
Observers	#1407 Eventual hindlimb	#1470 Pure hindlimb	#1449 Pure forelimb
A vs. B	0.82	0.69	1.00
A vs. C	0.82	0.82	0.83
A vs. D	0.82	0.81	0.83
A vs. E	0.82	0.70	0.69
B vs. C	1.00	0.83	0.83
B vs. D	1.00	0.53	0.83
B vs. E	1.00	0.66	0.69
C vs. D	1.00	0.64	1.00
C vs. E	1.00	0.82	0.54
D vs. E	1.00	0.81	0.54

TABLE III. Clinical Types of hSOD1 (G93A) Transgenic Rats

Clinical type	Subtype	*n*	%
Forelimb	Pure	4	8.2
	Eventual	5	10.2
Hindlimb	Pure	19	38.7
	Eventual	17	34.7
General		4	8.2
Total		49	100

Real-Time RT-PCR and Western Blot Analysis

Tissue specimens were dissected from the cerebral cortices, cerebella, medullae, and spinal cords (cervical, thoracic, and lumbar spinal cords) of the deeply anesthetized rats, and divided into two portions for total RNA and total protein preparation. Total RNA was isolated and first strand cDNA was synthesized as described previously (Okada et al., 2004). The real time RT-PCR analysis was carried out using Mx3000P (Stratagene, La Jolla, CA) with SYBR Premix Ex Taq (Takara Bio, Inc., Otsu, Japan). The primers used for the analysis were human *SOD1* (5′-TTGGGCAATGTGACTGCTGAC-3′, 5′-AGCTAGCAGGATAACAGATGA-3′), rat *SOD1* (5′-ACTTCGAGCAGAAGGCAAGC-3′, 5′-ACATTGGCCACACCGTCCTTTC-3′), and *β-actin* (5′-CGTGGGCCGCCCTAGGCACCA-3′, 5′-TTGGCCTTAGGGTTCAGAGGGG-3′). The results are presented as ratios of mRNA expression normalized to an inner control gene, *β-actin.* Total protein was prepared in lysis buffer containing 10 mM Tris-HCl (pH 7.6), 50 mM NaCl, 30 mM sodium pyrophosphate, 50 mM sodium fluoride, 20 mM glycerophosphate, 1% Triton X-100, and a protease inhibitor mixture (Complete; Roche Applied Science, Mannheim, Germany). Western blot analysis was carried out by a method established previously. In brief, a 5 μg protein sample of an extract was run on 12% SDS-PAGE, transferred to nitrocellulose, and probed with anti-human SOD1 (1:1,000, mouse IgG, Novocastra Laboratories, Ltd., Benton Lane, UK), and anti-α-tubulin (1:2,000, mouse IgG, Sigma-Aldrich, Inc., Saint Louis, MO). Signals were detected with HRP-conjugated secondary antibodies (Jackson ImmunoResearch Laboratories, Inc., West Grove, PA) using an ECL kit (Amersham Bioscience UK limited, Little Chalfont, UK). Quantitative analysis was carried out with a Scion Image (Scion Corporation, Frederick, MD). The amounts of proteins loaded in each slot were normalized to those of α-tubulin.

Immunohistochemical Analysis

Rats were deeply anesthetized (ketamine 75 mg/kg, xylazine 10 mg/kg, i.p.) and transcardially perfused with 4% paraformaldehyde/PBS (0.1 M PBS, pH 7.4) for histological examination. Spinal cord tissues were dissected out and postfixed overnight in the same solution. Each spinal cord was dissected into segments that included the C6, T5, and L3 levels, immersed in 15% sucrose/PBS followed by 30% sucrose/PBS at 4°C, and embedded in Tissue-Tek O.C.T. Compound (Sakura Finetechnical Co., Ltd., Tokyo, Japan). Embedded tissue was immediately frozen with liquid nitrogen and stored at −80°C. Serial transverse sections of each spinal segment were cut on a cryostat at a thickness of 14 μm. The sections were pre-treated with acetone for 5 min, rinsed with PBS three times and permeabilized with TBST (Tris-buffered saline with 1% Tween 20) for 15 min at room temperature. After being blocked in the TNB buffer (Perkin-Elmer Life Sciences, Inc., Boston, MA) for 1 hr at room temperature, the sections were incubated at 4°C overnight with an anti-choline acetyltransferase (ChAT) polyclonal antibody (AB144P, Goat IgG, 1:50; Chemicon International, Inc., Temecula, CA). After being washed with PBS three times, the sections were incubated for 2 hr at room temperature with a biotinylated secondary antibody (Jackson ImmunoResearch Laboratories, Inc.). Finally, the labeling was developed using the avidin-biotin-peroxidase complex procedure (Vectastain ABC kits; Vector Laboratories, Inc., Burlingame, CA) with 3,3-diaminobenzidine (DAB; Wako Pure Chemical Industries, Ltd., Osaka, Japan) as the chro-

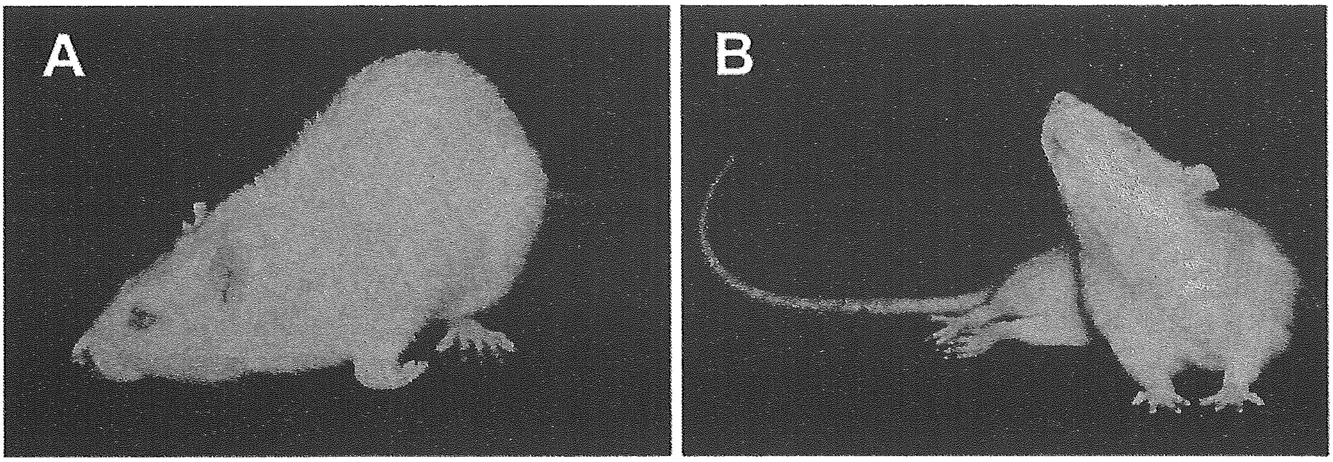

Fig. 2. Characteristic appearance of hSOD1 (G93A) transgenic rats. **A:** Forelimb type. The rat was unable to raise its head and was obligated to take a posture of raising the lumbar region, as indicated, because of the paralyzed forelimbs. **B:** Hindlimb type. The rat showed paraplegia, but was able to raise its head and upper trunk with its non-paralyzed forelimbs.

mogen. Immunohistochemical images were examined with a Zeiss-AxioCam microscope system.

Motor neurons bearing ChAT-immunoreactivity in laminae VII, VIII, and IX of the ventral horn were counted in every tenth section (5 sections total for each segment) for each of the C6, T5, and L3 segments. Only the neurons that showed labeling above background level and were larger than 20 μm in diameter were counted. The numbers of motor neurons in all segments (C6, T5, and L3) were summed for each animal to evaluate not only the local motor neuron loss, but the generalized loss of motor neurons throughout the spinal cord of each animal ($n = 3$ for each genotype at each time point). We next examined the correlation between the number of residual motor neurons and the results of the functional analyses described in this study. Statistical analysis was carried out with two-tailed unpaired Student's *t*-test. A *P*-value of <0.05 was considered statistically significant.

RESULTS

Clinical Types of hSOD1 (G93A) Transgenic Rats

Because we noticed variations in the disease phenotypes expressed by the G93A rats, we classified 49 rats into three clinical categories according to the location of initial paralysis. The clinical types were: the forelimb type, hindlimb type, and general type (Table III). Rats whose paralysis started in the forelimbs and progressed to the hindlimbs were defined as the "forelimb type." In contrast, rats whose paralysis started from the hindlimbs and progressed to the forelimbs were defined as the "hindlimb type." A typical appearance for the forelimb and hindlimb types is shown in Figure 2. Other rats, which showed simultaneous paralysis in the forelimbs and hindlimbs, were categorized as the "general type".

In addition, we classified the forelimb- and hindlimb-type rats into two subtypes, the pure and eventual types, based on the timing of the initial paralysis (Table III). Rats of the pure type showed paralysis that was limited to one or more of the four limbs as the initial observable deficit. Those of the eventual type initially showed symptoms of general muscle weakness (e.g., walking with a limp, sluggish movement), but without unequivocal limb paralysis. In the eventual type animals, paralysis of one of the limbs became apparent later. The ratio of each subtype is shown in Table III.

Evaluation of Disease Progression in the hSOD1 (G93A) Transgenic Rats

Although the transgenic rats varied in their clinical types, all four measures of disease progression (body weight, inclined plane test, cage activity, and SCANET) showed significant differences between the transgenic and wild-type rats (Fig. 3).

In contrast to the continuous weight gain in wild-type rats, the body weight in the affected rats ceased to increase and gradually decreased, with peak body weight attained around 110–120 days of age ($P < 0.05$, after 112 days of age) (Fig. 3A).

In the inclined plane test, initially both the transgenic and wild-type rats uniformly scored 75–80 degrees, after several training trials. However, the transgenic rats showed a significant decline in performance compared to their wild-type littermates from 120 days of age (Fig. 3B).

In the cage activity measurement, the movements of the wild-type rats remained stable, whereas those of the transgenic rats declined rapidly after 125 days of age (Fig. 3C).

In the SCANET test, even the wild-type rats showed decreased movements for all parameters (M1, M2, RG) in the late observation period, though they showed no abnormality in their motor functions. This might be because they had acclimated to the SCANET cage. The movement score of the transgenic rats was consistently worse than that of the wild-type rats after